Spread and Control of Rift Valley Fever virus after accidental introduction in the Netherlands. A modelling study.

Fischer E.A.J., Boender G.J., de Koeijer A.A., Nodelijk H.A., van Roermund H.J.W.
Central Veterinary Institute (CVI), part of Wageningen UR,
Lelystad, The Netherlands

Concept-rapport
BO-project BO-08-010-022
Looptijd 2009-2011

CVI projectnummer:
1691056100 (2009-2010) en 1635015600 (2011)

CVI-rapportnummer:
11/CVI0040

January 2012

Contents

Contents 2
Summary 3
1. Introduction 6
2. The Mathematical Model 7
2.1. Basic assumptions and applications of the model 7
2.2. Model description 9
2.3. Quantification of the model 12
3. Application of the model 21
3.1. Risk maps 21
3.2. Uncertainty analysis 22
3.3. Control measures: vaccination, culling and vector control 23
3.4. *Stomoxys calcitrans* and *Anopheles macullipennis* 24
3.5. Nature reserve 'De Oostvaardersplassen' 25
4. Results 26
4.1. Risk maps 26
4.2. Uncertainty analysis of the mathematical model 31
4.3. Effect of control measures 32
4.4. *Stomoxys calcitrans* and *Anopheles macullipennis* 39
4.5. Nature reserve 'De Oostvaardersplassen' 43
4.6. Surveillance and collection of data during an epidemic 44
5. Discussion 45
5.1. Risk maps 45
5.2. The mathematical model & uncertainty analysis 45
5.3. Effect of control measures 47
5.4. *Stomoxys calcitrans* and *Anopheles macullipennis* 49
5.5. Nature reserve 'De Oostvaardersplassen' 49
6. Conclusions 50
Acknowledgements 51
References 52
Appendix: Floquet formalism 57

Summary

Rift Valley Fever (RVF) is a zoonotic vector-borne infection and causes a potentially severe disease in both humans and young animals. Many mammals are susceptible to infection including important livestock species. Although currently confined to Africa and the near-East, this disease causes concern in countries in temperate climates where both hosts and potential vectors are present, such as the Netherlands. Currently, an assessment of the risk of an outbreak occurring in the Netherlands is missing.

The Ministry of Economic Affairs, Agriculture and Innovation (EL&I) is interested in the risk of an outbreak of Rift Valley Fever virus (RVFV) for the Netherlands, and more knowledge is needed about the risk of introduction of the virus, the risk of spread (transmission) of the virus in the country once introduced, and the methods for control and surveillance. For this purpose project BO-08-010-022 'Prevention and control of RFV in the Netherlands' was initiated in November 2008.

Objectives

To gain knowledge about the risk of introduction of RVFV in the Netherlands, the risk of spread of the virus in the country once introduced, and the methods for control and surveillance. This knowledge will assist the Ministry of Economic Affairs, Agriculture and Innovation (EL&I) in developing a suitable contingency plan for the (until now) unknown infection Rift Valley fever.

Research questions

(1) What are the introduction routes of RVFV in the Netherlands ?
(2) What is the transmission of the virus after accidental introduction in the country ?
(3) Which control measures are possible ?
(4) Where does a surveillance system have to be aimed at ?
(5) What are the relevant data which have to be collected during an epidemic ?

Research question (1) risk-analysis of introduction routes of RVFV in the Netherlands, is described in a separate report by Hoek et al [1]. The current report describes the results of questions (2) to (5) of this project.

Approach

A mathematical model was developed to study virus transmission in several livestock and vector species in the Netherlands. The model was parameterized using literature on parameters for host, vector and pathogen. The relative abundances of vectors (in 5 by 5 km grid cells of the Netherlands) were obtained by extrapolation of Belgium data to the Dutch climate and geography. The host densities were obtained from a database of 'Dienst Regelingen' of the Ministry of EL&I.

The parameterized model was used to determine the initial and long term epidemic growth rate of the virus, which are indicators of the probability of an outbreak and of persistence of RVFV. With these results, risk maps of the country were created, showing the areas at risk for a RVFV outbreak (if introduced) and for persistence of the infection. Uncertainty analysis yielded knowledge about important input parameters (for model output) and data gaps, on which we can focus in future research.

Results

Risk maps

Several areas of the Netherlands have a high transmission (spread) potential and a high risk of persistence of the infection. Counter-intuitively, these are the sparsely populated livestock areas, due to the high vector-host ratios in these areas.

Mosquito species *Culex pipiens* s.l. is found to be the main driver of the spread and persistence, because it is by far the most abundant mosquito in the Netherlands. Furthermore, outbreaks are more likely to occur in Summer and Autumn than in Spring, due to high vector abundances.

Uncertainty analysis

Vertical transmission of the virus from adult *Aedes vexans* vectors to eggs has almost no effect on an outbreak and even not on persistence of the infection, because of the minor role of this vector species in the transmission in the Netherlands.

For the mosquito abundances we used mosquito trap catches from Belgium, which were extrapolated to the Netherlands using landscape, vegetation, temperature, precipitation and soil data similarities. The model was found to be most sensitive to uncertainties in this parameter. Thus, accurate estimates of vector abundances for the Netherlands itself are needed.

Control measures

During past outbreaks of CSF, FMD and HPAI all animals on detected farms were culled, and preventive ring culling of animals around the detected farms was done to prevent spread to other farms. This ring culling policy will probably be changed for CSF and FMD to ring vaccination. The current policy in the Netherlands for RVF (Concept-Beleidsdraaiboek Rift Valley fever version 1.0, 2009) is culling of all ruminants on infected farms, and ring culling is not mandatory.

According to the current study, culling of livestock can have both positive and negative effects on the course of a RVF outbreak. Firstly, a negative effect of culling is the increase of the vector-host ratio in the area. The increased vector-host ratio increases the epidemic growth rate in the remaining host population. Secondly, by culling and thus removing livestock from an area, vectors might be more prone to search longer for hosts, hence increasing the infection pressure for populations in other areas (i.e. herds) or other less preferred hosts (i.e. humans). Positive effects of culling is the removal of infectious hosts, thus decreasing the average infectious period of hosts. This can reduce the epidemic growth rate, and indeed in our simulations culling shortens the duration of an RVF outbreak during the early season (May), but only when the delay between virus introduction and detection is short (10 days). When the epidemic growth rate is high (like in July), culling has no effect on an outbreak and other negative effects can have the overhand.

A more detailed investigation of the effects of culling during outbreaks of vector-borne diseases is done in another modelling study [2]. This study has shown that the outcomes of culling are at least unpredictable and therefore this strategy should be reconsidered.

If vaccination is chosen as intervention strategy, a high vaccination degree of more than 90% of animals (protected from infection) is needed to prevent RVF outbreaks throughout the year. Vector control (by larvicides or adulticide) can be a helpful tool to reduce the epidemic growth rate of RVF. However, when vector control is not combined with other intervention measures, very high reductions of

vector populations of more than 90% are needed to prevent an outbreak and persistence of the infection.

Stomoxys calcitrans and *Anopheles macullipennis*
The stable fly *Stomoxys calcitrans* also poses a potential risk for a RVF outbreak, if this mechanical vector is able to transmit RVFV as efficiently between livestock as experimentally shown between hamsters. Very low densities of this vector like one or two per cow are able to support a local outbreak on a farm.

As the mosquito *Anopheles macullipennis* was recently found associated with sheep in the Netherlands, we studied whether this species could act as the sole vector. However, *An. macullipennis* is not likely to be the driver of an epidemic in the Netherlands, as only in a few small areas this vector is able to support persistence of RVF.

Nature reserve
In a wetland nature reserve like 'de Oostvaardersplassen' with free ranging cattle and deer, an outbreak and persistence of RVFV can occur when either (1) deer species are a competent host for RVFV (like cattle), or when (2) the vectors do not bite deer (but only cattle). To our knowledge no deer species have been tested for RVFV competence and the preference of vectors for deer is unknown.

Recommendations

- The model output is strongly correlated with the estimated vector abundances. As vector trap catches from the Netherlands were not available, observed data from Belgium were extrapolated and used for this study instead of real Dutch data. This gap in knowledge must be solved by vector monitoring in the Netherlands (by Centre Monitoring Vectors, Wageningen).
- The RVFV competence of Dutch vector species is unknown. The main focus of vector-competence studies should be addressed to species associated with livestock and/or wildlife and present in high abundances. *Culex pipiens s.l.* contributes by far most to the spread and persistence of RVFV in the Netherlands, according to the model. Further studies on vector competence for RVFV, abundance and host preference of *Cx. pipiens* s.l. in the Netherlands are most important to decrease the amount of uncertainty in the model.
- The effect of culling is unpredictable with vector-borne infections and therefore this strategy should be reconsidered. Other control strategies should be assessed further. Combined strategies like emergency vaccination and vector-control are most likely to be feasible.
- In order to assess the RVF risk in wildlife populations in the Netherlands, the host competence of deer species for RVF and the vector-preference for deer should be determined.
- Wildlife, such as deer and rodents (especially rats), can be a reservoir of RVFV and surveillance during an outbreak is warranted.
- Monitoring of all biting arthropods, such as mosquitoes, midges, stable flies and ticks, present in the stable or meadow of infected farms should be done during a RVF outbreak.

1. Introduction

Rift Valley Fever virus (RVFV; Bunyaviridae: Phlebovirus) is primarily transmitted by mosquitoes and causes a potentially severe disease among both humans and animals. Many mammals are susceptible to infection, though particularly farm animals such as cattle, sheep and goats are affected. RVF infection causes abortion in pregnant animals and high mortality rates of newborns. In older animals, infection is generally milder and may even be asymptomatic. Extensive reviews can be found in [3, 4].

Humans can become infected with RVF following contact with infected animals or animal products or as a result of a mosquito bite. RVF infection in humans is generally mild or unapparent with low mortality rates (<1%) ([4, 5]. However, mortality rates vary markedly from one outbreak to another and were high among confirmed cases (14%) during a large epizootic in Yemen and Saudi Arabia in 2000 [4, 6] . The most common complications following RVF infection in humans are optic atrophy (3-4%), meningo-encephalitis (<1%), and viral hemorrhagic fever (<1%) [7]

The virus was first isolated during an outbreak in the 1930's in the Rift Valley of Kenya, hence the name [8]. Between 1930 and 1977 outbreaks of RVFV were limited to sub-Saharan Africa. In 1977 the first documented outbreak north of the Sahara was documented in Egypt and in 2000 the first outbreak occurred outside the African continent on the Arabian Peninsula in Saudi Arabia and Yemen [3].

Introduction of RVFV into new areas will mainly be caused by the international trade in live domestic animals and by the unintended transport of vectors on airplanes and sea vessels [1]. These transports are very much intensified during the last decade. Due to the presence of competent vector species in RVF-free regions [9-11] and the possible introduction of new vector species which may persist in the new area due to climate changes, we studied the transmission possibilities of RVFV after accidental introduction in the Netherlands.

For this purpose, a mathematical model was developed to study (1) the probability of a RVF outbreak at different days of introduction during the year, (2) the probability of persistence of the infection during the entire year, and (3) outbreak size and duration at different days of introduction during the year. With the model, risk maps of the country were created, showing areas at risk for a RVF outbreak and for persistence of the infection. Uncertainty analysis yielded knowledge about important input parameters (for model output) and data gaps, on which we can focus in future research.

2. The Mathematical Model

2.1. Basic assumptions and applications of the model

The spread of RVFV after introduction in the Netherlands is assessed using a deterministic mathematical model. This model describes the local spread of the infection. Local spread means the transmission of RVFV in a predefined small area, in which all hosts and vectors mix homogeneously within this area. In this report we have used 5 by 5 kilometre areas, which is equivalent to an intervention area of 3 km radius around an infected farm.

The model is developed and subsequently applied for three different calculations: (1) initial spread of the infection for all cells of a 5 by 5 km grid, (2) persistence of the infection for all cells of a 5 by 5 km grid, and (3) the time course of an outbreak for selected areas.

Initial spread of the infection is possible if the epidemic growth rate ($time^{-1}$) at a certain moment during the year is larger than 0. A growth rate larger than 0 means that the number of infected hosts and vectors is growing immediately after introduction of the virus, and this determines the potential of an outbreak. This quantity is calculated for Dutch conditions at different time-points during the year.

Persistence of the infection is calculated by a method to average the initial growth rates (in $time^{-1}$) at all time-points over one year. The methodology to calculate this quantity is based on the Floquet theory and the exact mathematics are described in Appendix I. The principle idea behind the method is that an infection can only persist over multiple years, if the overall average growth rate during a year is larger than 0.

Finally, the model is used to simulate the time course of outbreaks, i.e. the time course of infected hosts and vectors at different starting points in the year. The model is deterministic, which means that the outcomes represent the *average* field situation.

The behaviour of mosquitoes during winter months (diapause) and how that affects the virus survival, is poorly understood. Here we assume a period of stasis during winter. This means that we assume that the number of susceptible, infected and recovered hosts and the number of susceptible and infected vectors at the beginning of the vector season is equal to the situation at the end of the previous vector season. This implies that the infection does not die out during the winter.

The vector season is defined here as the period during which vectors are active. Active vectors have a biting rate larger than 0. For the vectors in this model, the vector season is between 21st of April and 23rd of October, based on average daily (24h) temperatures in the Netherlands (of 1971-2000, KNMI) and the temperature threshold for biting of 9.6 ºC [12].

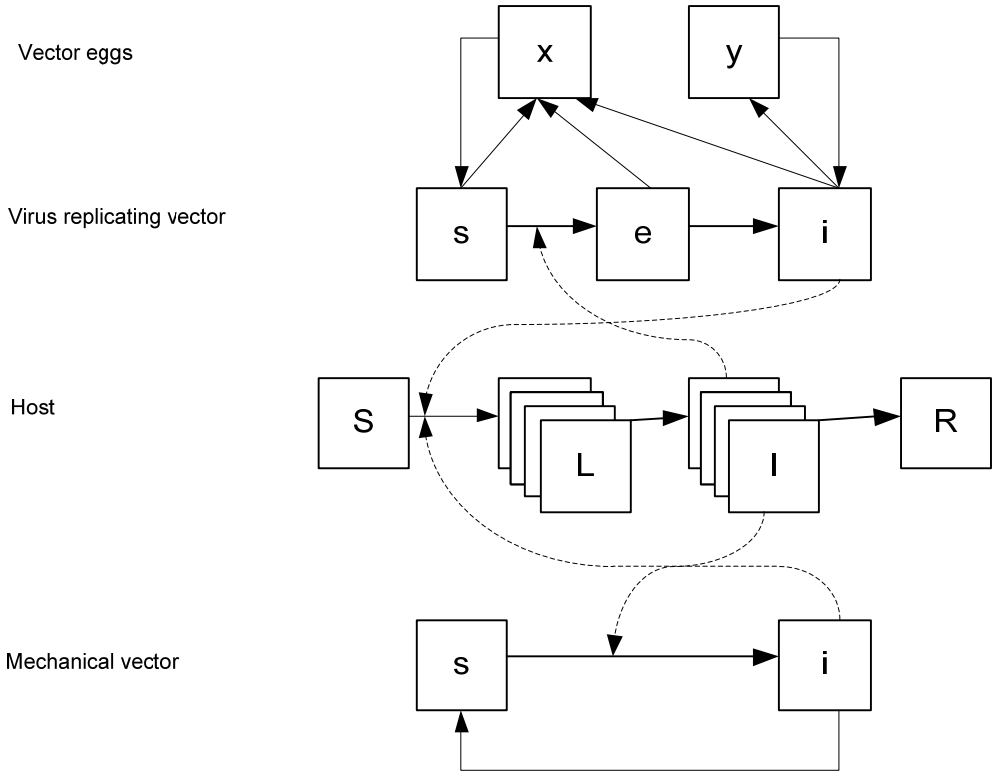

Figure 1. Schematic flowchart of the model. For abbreviations, see text.

2.2. Model description

The core of the model is a set of coupled ordinary differential equations abbreviated ODEs (Equations 1-16). Figure 1 is a flowchart of the model for a more visual representation. Hosts are categorized into 4 states: **S**usceptible, **L**atent, **I**nfectious and **R**ecovered. The latent and infectious state is divided into sub-classes to allow for a gamma-distributed infectious period [13].

Host

$$\frac{dS_j^h}{dt} = -\sum_{i=1}^{m}\left(\Lambda_{ij}^h b_i(t)\,\frac{S_j^h}{N_j^h}\,I_i^v\right) + \mu_j^h(N_j^h - S_j^h)$$

$$\frac{dL_j^h}{dt} = \sum_{i=1}^{m}\left(\Lambda_{ij}^h b_i(t)\,\frac{S_j^h}{N_j^h}\,I_i^v\right) - (\phi_j^h + \mu_j^h)L_j^h$$

$$\frac{dI_j^1}{dt} = \phi_j^h L_j^h - (\gamma_j + \mu_j^h)I_j^1$$

$$\frac{dI_j^g}{dt} = \gamma_j I_j^{g-1} - (\gamma_j + \mu_j^h)I_j^g$$

$$I_j^h = \sum_{i=0}^{k_j} I_j^i$$

$$\frac{dR_j^h}{dt} = \gamma_j I_j^k - \mu_j R_j^h$$

Equations 1-6

Equations 1-6 describe the dynamics of the infection in hosts of species *j*, in which superscript *h* indicates that the variable depicts a host (and likewise, superscript *v* depicts a variable representing a vector). We start the explanation with the simplest Equations 3-6 describing the *k* infectious classes (*I*) and the recovered class (*R*). Latently infected hosts (*L*) enter the first infectious class from the latent class with a transition rate ϕ_j^h, and leave each infectious class with transition rate γ_j^h to the next infectious class or they die with rate μ_j^h. The hosts in the last infectious class *k* enter into the recovered state. The hosts remain in this state until they die, and are replaced by birth of new susceptible animals.

More complicated is the calculation of the transmission rate which is the rate at which hosts are infected, thus transit from the susceptible (*S*) to the latent class (*L*). This rate is given by the rather cryptic factor $\sum_{i=1}^{m}\left(\Lambda_{ij}^h b_i(t)(S_j^h / N_j^h)\cdot I_i^v\right)$, which sums the infection pressure from all infected vectors of *m* vector species. This summation includes the number of infectious vectors I^v_j and the fraction of susceptible hosts S_j^h / N_j^h, the biting rate $b_i(t)$ of vector *i* and the term Λ_{ij}^h. The term Λ_{ij}^h is the *host specific per bite transmission* from vector *i* to host *j*, which is defined as the fraction of successful transmission events from one infected vector of species *i* to a host of species *j* per bite.

$$\Lambda_{ij}^{h} = \alpha_{ij} \cdot p_{ij}$$
$$= \alpha_{ij} \frac{\pi_{ij} N_j^h}{\sum_{k=1}^{n} \pi_{ik} N_k^h}$$

Equation 7

This term includes the transmission probability from vector species *j* to host species *i*, α_{ij}, and the probability of biting a host of species *j*, p_{ij}. The probability of biting a host of species *j* is calculated by multiplication of the preference for host *j* by vector species *i*, π_{ij}, with the number of hosts of species *j* (N_j), divided by the sum of all preferences times host population sizes. We emphasize that the preferences *and* host population sizes determine the distribution of bites of a certain vector species over the host species. The biting rate (number of bites per vector-individual per day) is not affected by the number of hosts nor is the composition of hosts of influence on the biting rate of an individual vector.

A distinction is made between three types of vectors: vectors in which the virus replicates (from now on called virus replicating vectors) with vertical transmission, virus replicating vectors without vertical transmission and mechanical vectors. For virus replicating vectors such as mosquitoes, only females play a role in transmission, because they need a blood-meal for egg maturation, and the males do not. For mechanical vectors such as the stable fly, both males and females are important for transmission, because both sexes use blood for maintenance.

Uninfected vectors are all **S**usceptible. Virus replicating vectors have an extrinsic incubation period (**L**atent period) in which they cannot infect hosts, and subsequently an **I**nfectious state. The infected vectors remain infectious until death. A fraction of eggs of infectious vertical transmitting vectors will become infected eggs and, after hatching and passing through larval states, develop into infectious females; these eggs form an extra infectious state ***Y*** (see Figure 1). The dynamics of these vectors are then described by the following equations.

Vector in which the virus replicates (virus replicating vector)

$$\frac{dN_j^v}{dt} = h_j(t) - \mu_j^v(t) N_j^v$$
$$\frac{dY_j}{dt} = \varsigma_j c_j b_j(t) I_j^v - h_j(t) \frac{Y_j}{G_j}$$
$$\frac{dS_j^v}{dt} = -\sum_{i=1}^{n} \left(\Lambda_{ij}^v b_j(t) S_j^v I_i^h \right) + h_j(t) \frac{G_j - Y_j}{G_j} - \mu_j^v(t) S_j^v$$
$$\frac{dL_j^v}{dt} = \sum_{i=1}^{n} \left(\Lambda_{ij}^v b_j(t) S_j^v I_i^h \right) - (\mu_j^v(t) + \phi_j^v(t)) L_j^v$$
$$\frac{dI_j^v}{dt} = h_j(t) \frac{Y_j}{G_j} + \phi_j^v(t) L_j^v - (\mu_j^v(t) \cdot d_j^v) I_j^v$$

Equations 8-12

The first equation gives the vector-population dynamics. N^v_j is the population size of vector *j*. The vector population size depends on the number of new adult vectors entering the population, $h_j(t)$, and the mortality of vectors $\mu^v_j(t)$.

The number of eggs is difficult to observe and no data is available. To incorporate infected eggs in the model we made some simplifying assumptions: (1) we only model eggs that will eventually develop into an adult (egg, larval and pupal mortality is not explicitly modelled), (2) the number of eggs is approximately constant in time, (3) following from the above two assumptions, the number of eggs produced equals the number of hatching adults during a year, such that the adult vector population size remains equal each year. Using these simplifications of the dynamics of the eggs and adult vector population, we model the impact of vertical transmission.

Infectious vertical transmitting virus replicating vectors produce infected eggs with a probability ς_j. The rate at which one female produces eggs, is determined by the biting rate *b(t)* and the batch size c_j. The batch size, c_j, is determined in the model such that the vector population remains equal for each year (see assumption (1) and (3)). The eggs hatch with a number of $h_j(t)$ at time *t*. The population dynamics of the eggs is not explicitly modelled, because this would unnecessarily complicate the model. To determine the fraction of infected (hatching) eggs, we assume that the egg population is constant during the year at size G_j (see assumption (2)). The size of the egg population G_j is estimated by the inverse of the mean survival time of an egg multiplied by the maximum vector population abundance, i.e. the peak abundance during the season. For non-vertical transmitting vectors, the eggs are disregarded in the model.

Different from that in hosts, the infectious state of virus replicating vectors is ended by death of the vector alone. Some vectors will have a mortality rate increased with a factor d_j^v due to infection.

Mechanical vectors are different from the virus replicating vectors in two ways. Firstly, mechanical transmitting vectors are infectious immediately after becoming infected during a blood meal on an infectious host, i.e. there is no extrinsic incubation period, and secondly, they recover from the infection after a short period, with rate σ_j.

Mechanical vector

$$\frac{dN_j^v}{dt} = h_j(t) - \mu_j^v(t)N_j^v$$

$$\frac{dS_j^v}{dt} = -\sum_{i=1}^{n}\left(\Lambda_{ij}^v b_j(t)S_j^v I_i^h\right) + \sigma_j I_j^v + h_j(t) - \mu_j^v(t)S_j^v$$

$$\frac{dI_j^v}{dt} = \sum_{i=1}^{n}\left(\Lambda_{ij}^v b_j(t)S_j^v I_i^h\right) - (\mu_j^v(t) + \sigma_j)I_j^v$$

Equations 13-15

The transmission rate to vectors is determined by the summation of infection by different host species. This calculation includes the number of infectious hosts I^h_j and the number of susceptible vectors, the biting rate $b_i(t)$ of vector *i* and the term Λ_{ij}^v. This factor, Λ_{ij}^v, is the *per bite transmission* from *one* infected individual of host *j* to a susceptible individual of vector *i*, which is defined as the fraction of successful transmission events during one bite on a random host of species *j* by a random vector of species *i*.

$$\Lambda_{ij}^{v} = \beta_{ij} \cdot p_{ij} \cdot \frac{1}{N_j^h}$$

$$= \beta_{ij} \frac{\pi_{ij}}{\sum_{k=1}^{n} \pi_{ik} N_k^h}$$

Equation 16

In Equation 16 β_{ij} is the transmission probability from host to vector during one bite. The probability of biting a host of species *j* by vector species *i* is p_{ij}. This probability depends on the vector preference and host abundances (see Equation 7 and accompanying text). The probability of biting the *one* infectious host is given by dividing with the host population size: $1/N_k^h$.

Several parameters of the vector are not constant in time; the biting rate *b(t)*, mortality rate $\mu_j^v(t)$ and rate of transition from the extrinsic incubation period $\phi_j^v(t)$ in the model change with time *t* due to the temperature dependence of these parameters. The temperature dependence is modelled using the average daily (24 h) temperature at the centrally located meteorological institute in De Bilt, the Netherlands [14]. Hatching rate $h_j(t)$ is the number of eggs hatching at a certain moment in time. This function is time dependent and inferred from the expected population size of the vector (more precise, the virus replicating vector with vertical transmission), as explained earlier.

2.3. Quantification of the model

2.3.1. Host

Selection of host species

Many African mammalian species are susceptible to infection with RVFV. The wide variety of species includes cattle, goat, sheep [8, 15], but also wildlife such as giraffe and African buffalo [16, 17]. Birds and reptiles are refractory, also for the Netherlands important livestock species pigs [18], horses and other equines are resistant to the infection [4, 19].

The focus of this report is on disease transmission in livestock. The host species under consideration in the current study (to create risk maps of the Netherlands) are domestic livestock: cattle, sheep and goat. Pigs and equines can only be infected at extremely high inoculation doses impossible to achieve through vector-borne transmission, and are therefore not taken into account. Other animal species, such as rodents, deer and other wildlife, are not taken into account, because they are either assumed to play a minor role in the epidemiology (rodents [19]), or because their susceptibility is unknown (deer species). Also humans are assumed not to play a role in the epidemiology of RFV in livestock species. Some considerations for humans can be found in the report of the Emerging Zoonoses project [20].

Free range cattle is not included, as their numbers in the Netherlands are relatively low compared to domesticated cattle. However, free range cattle is included to study the epidemiology in special areas such as nature reserves (Oostvaardersplassen). Free range cattle is assumed to have the same infection characteristics as domesticated cattle. In this part of the study, we will assume that deer are either non-competent animals, or have the same infection biological characteristics as cattle.

Parameters estimates

Cattle becomes viraemic after 1 to 2 days post infection. The viraemia peaks at 2 to 5 days post infection [4, 18]. The viraemia remains detectable up to 7 days, but for calves 5.9 days on average in a study by McIntosh [21].

For Nigerian sheep breeds fever and viraemia was found after 24 hours, which remained present up to 7 days. The sheep of one breed (Yankasa) all died during the viraemic period [22]. Lambs younger than one week at infection showed viraemia after 16 hours and died between 36 and 42 hours [4, 18]. Older lambs were viraemic for up to 3 days, and at the next sample 7 days later they were negative [21]. In older sheep and goat, viraemia was found 1 to 2 days after inoculation, also peaking at 2 to 5 days. The virus was detectable up to 7 days [4, 18, 23].

For the calculations we consider the latent period and the infectious period of cattle, sheep and goat to be equal. Overall, the data imply that the latent period is 1 day and the infectious period is 5 days with a variance of 1.25 days (Table 1).

Table 1. Estimated host parameters and their range (used in the uncertainty analysis). See Equations 1–16.

Parameter	Definition	Value	Unit	Range
$1/\varphi^h$	Average latent period of host	1	day	(0 – 2)
γ^h	Transition rate infectious classes	0.25	day^{-1}	(0.07 – 0.67)
k	Number of infectious classes	20	-	(5 – 98)
$\gamma^h * k$	Mean infectious period	5.0	day	(3.0 – 7.0)
$(\gamma^h)^2 * k$	Variance infectious period	1.25	day^2	(0.5 – 2.0)
$1/\mu^h_{cattle}$	Life expectancy cattle	1095	Day	–
$1/\mu^h_{sheep\&goat}$	Life expectancy sheep & goat	1095	day	–

2.3.2. Vector

Selection of vector species

Initially, five vector species were taken into account for the Netherlands: the mosquito's *Aedes vexans vexans*, *Ochlerotatus caspius*, *Aedes cinereus* s.l., *Culex pipiens* s.l. and the stable fly *Stomoxys calcitrans*. Three of these species, *Ae. vexans vexans*, *O. caspius* and *Cx. pipiens* s.l., were indicated by an EFSA report as potential vectors in the Netherlands and Belgium [19]. Due to a lack of data on *O. caspius,* the population abundance could not be estimated for these countries [24]. However, it is clear that the abundance of this species is very low, and including or excluding does not affect the outcomes of the model. *Ae. cinereus* s.l. has never been tested for RVFV vector competence, and is added as vector species to test the sensitivity of the study to an unrecognized extra vector.

Two of the Dutch potential vector species are part of a species complex: *Aedes vexans vexans* and *Culex pipiens* s.l. *Ae. vexans vexans* is the European sub-species of *Ae. vexans.* Another sub-species *Ae. vexans arabiensis* was a major vector in the Saudi-Arabian outbreak [25]. In this study we assume that the Dutch *Ae. vexans vexans* has the same vector competence as *Ae. vexans arabiensis* and we will from now on call this species *Aedes vexans*. The situation for *Cx. pipiens* s.l. is more complex. The main two sub-species *Cx. pipiens* s.s. and *Cx. pipiens molestus* differ in host-preference. *Cx. pipiens* s.s. is strictly ornithophilic and will not bite mammals,

while *Cx. pipiens molestus* is opportunistic and bites both birds and mammals. The sub-species hybridize to form populations with intermediate preferences. For Dutch species it is unknown which species or hybrid is present (pers. comm. E.J. Scholte). In this study we assume that *Cx. pipiens* s.l. is purely biting on mammals (livestock).

In a separate application of the model we will pay attention to the impact of two additional vector species, the stable fly *Stomoxys calcitrans* and the sheep-associated mosquito *Anopheles macullipennis*, on the epidemiology of RVF in the Netherlands. *S. calcitrans* is a stable fly and not a mosquito. This species can mechanically transmit the RVFV virus from one host to another [26], but RVFV has never been found on this vector during RVF epidemics. This is probably due to the short period in which the fly carries the virus, approximately 24 h [26]. As this species is very abundant in stables in the Netherlands and bites frequently, a separate study is performed to assed the potential impact of this vector on the epidemic.

An. macullipennis complex is a complex of mosquito species which is found in sheep stables (pers. comm. E.J. Scholte). Members of this complex were found to transmit malaria while still indigenous in the Netherlands. The competence to transmit RVF was never tested. We will create risk maps for this species assuming they have the same parameter values as *Cx. pipiens* s.l. or as *Ae. vexans*.

In summary, three vector species, *Ae. vexans, Ae. cinereus* s.l. and *Cx. pipiens* s.l. are used to estimate the baseline probability of outbreaks and persistence for the Netherlands. Separate analyses are done for each of these species to determine their contribution to the risk of RVF. An additional assessment is made for the stable fly *S. calcitrans* and mosquito species *An. macullipennis*.

Parameter estimates

Survival studies indicate that, given a constant temperature, an exponential distribution of the longevity of mosquitoes (i.e. duration of adult stage) is a good description for *O. caspius* [27, 28]. This means that the longevity can be described by one parameter μ^v for each of the species, and the average longevity is $1/\mu^v$. This parameter does, however, change with temperature.

This average longevity of mosquitoes is negatively correlated with temperature, described by a linear decrease in longevity (see equations in Table 2). The longevity of both *Aedes* species is based on data at constant temperatures of 13ºC and 21ºC [29]. The longevity of *Cx. pipiens* s.l. is over 30 days at temperatures below 20ºC [30], declining to 10 or 14 days at 24-27 ºC [31]. Additionally, infection by RVFV increases the mortality rate of *Cx. pipiens* s.l. with 26% [32]. This is not the case for the other vector species.

Longevity of *S. calcitrans* has a more complex relation with temperature (see Table 2) and is experimentally determined [33] with an optimum of 40 days at 20°C. The end of the infectious period is, however, not determined by death of the fly but by clearance of the virus. The flies are able to transmit the virus up to 24 hours, and we used a mean of 0.5 day.

Mosquito females take a blood meal to develop eggs. Hence the time between two blood meals consists of the total time to mature eggs, to find a breeding site and to oviposit (laying eggs). This cycle is called the gonotrophic cycle. The maturation of the eggs is temperature dependent and the largest proportion of the gonotrophic cycle consists of maturation of the eggs. The length of the gonotrophic cycle for *Cx. pipiens* s.l. as function of temperature was estimated for laboratory and natural conditions [12]. For *Ae. vexans* several African and European estimates were made, but none report the temperature. However, the few available data points for *Ae. vexans*

correspond to the expected values from the function for the length of gonotrophic cycle for *Cx. pipiens* s.l., taking the long term daily average temperatures in the area of study [34-36]. Therefore, the biting rate for all mosquito species is taken equal. Mosquito biting activity seizes at 9.6 ºC [12].

The extrinsic incubation period (EIP) is the time between a blood meal on an infectious host and the first successful transmission from vector to host during another blood meal. The EIP depends on virus replication and external temperature. The length of the EIP is fitted to experimental data for *Cx. pipiens* s.l. [37-39] and *Ae. vexans arabiensis* [25]. The data for *Ae. vexans arabiensis* consisted of two data points measured at temperatures only a few ^{o}C apart, therefore the temperature dependence of the EIP could not be estimated. The same linear relation with temperature as for *Cx. pipiens* s.l. [37-39] was used (Table 2). *S. calcitrans* is infectious immediately after biting and has no EIP [26].

Table 2. Estimated vector parameters and their range (used in the uncertainty analysis), and their relationship with temperature *T* (24 h daily average in ^{o}C). See Equations 1–16.

Parameter	Definition	Value	Unit	Range
$1/\mu^{v}_{Aedes}$	Longevity of *Aedes* species $1/\mu^{v}_{Aedes}(T) = a_0 - a_1 T$	$a_0 = 25.8$ $a_1 = 0.45$	day	(11.1 – 46.8) (-0.37 –1.67)
$1/\mu^{v}_{Culex}$	Long. of Culex pipiens $1/\mu^{v}_{Culex}(T) = a_0 - a_1 T$	$a_0 = 69.1$ $a_1 = 2.14$	day	(-21.7 – 160.0) (-1.99 – 6.28)
d^{v}_{Culex}	Increased mortality of infected *Culex*	1.26		(1.00 – 1.50)
$1/\mu^{v}_{S.calcitrans}$	Longevity of *S. calcitrans:* $1/\mu^{v}_{S.calcitrans}(T) = a_0 - a_1 T - a_2/T$	$a_0 = 166.0$ $a_1 = 3.7$ $a_2 = 1078.5$	day	(149.0 – 183.0) (3.3 – 4.1) (936.2 – 1220.8)
$b_{mosquitoes}$	Biting rate of mosquito species $b(T) = b_{slope}(T- b_{min})$	$b_{min} = 9.60$ $b_{slope} =$ 0.0173	day^{-1}	(7.6 – 11.6) (0.0163 – 0.0183)
$b_{Stomoxys}$	Biting rate of *S. calcitrans*	1	day^{-1}	(0.5 – 2)
$1/\varphi^{v}_{Aedes}$	Extrinsic incubation period *Aedes* species: $\varphi(T) = \varphi_{max} - \varphi_{slope} T$	$\varphi_{max} = 18.9$ $\varphi_{slope} = 0.30$	day	(0.0 – 37.8) (-0.35 – 0.93)
$1/\varphi^{v}_{Culex}$	Extrinsic incubation period *Culex* species: $\varphi(T) = \varphi_{max} - \varphi_{slope} T$	$\varphi_{max} = 11.3$ $\varphi_{slope} = 0.30$	day	(0.0 – 22.6) (-0.35 – 0.93)
$\sigma_{Stomoxys}$	Recovery rate *S. calcitrans*	2	day^{-1}	(1.0 – 3.0)

2.3.3. Host-vector interactions

Host-vector interactions consist of the parameters described in Equations 7 and 16, which are transmission probabilities from vector to host α_{ij} and from host to vector β_{ij}, and the host preference of a vector π_{ij}. The estimates of the transmission probabilities are based on laboratory studies with mosquitoes and RVFV infected and uninfected hamsters. Host preference is based most preferably on choice experiments

with different host species, and if not available, on blood meal analysis. A blood meal analysis determines the content of the gut of a vector caught in a trap, hence showing on what hosts the vector has taken a blood meal. This only shows which hosts were bitten by the vector, and not necessarily the host preference of the vector. From blood meal analysis the preference of the vector cannot be determined, because the content of the gut is the result of a combination of host preference and host availability (i.e. host density).

Transmission probabilities

The transmission probabilities from host to virus replicating vector are determined as the fraction of disseminated infections after a blood meal. The probability of transmission from vector to host is determined where possible by transmission from vectors with disseminated infection. Virus isolation from the legs of arthropods (after disinfection of the outside) indicates that the infection has disseminated through the body of the vector. Transmission probabilities were estimated from literature, separately for *Aedes* species, *Culex pipiens* s.l. and *Stomoxys calcitrans* (see Table 3).

The transmission probabilities from and to *Aedes* species were determined by experiments with *Ae. mcintoshi, Ae. fowleri, Ae. taeniorhynchus* and *O. caspius*. Unfortunately, *Ae. vexans arabiensis* mosquitoes were tested in a pool such that the competence and not the transmission probability per bite could be calculated [25].

Transmission from host to *Aedes* ranged between 18% and 82%. Infection and dissemination was 30% for *Ae. fowleri*, 60% for *Ae. mcintoshi* [40] and 40% for *O. caspius* [41]. It was shown that rearing temperature had an effect for *Ae. taeniorhynchus,* with dissemination rates ranging from 18% and 60% [42]. *O. caspius* was infected (not clear whether disseminated or not) in 77.5% to 82.14% of the cases after one blood meal [43].

Transmission from *Aedes* to host ranged between 9.7% and 100%. *Ae. fowleri* with a disseminated infection fed on hamsters lead to 61% of these hosts being infected, and all hamsters were infected by *Ae. mcintoshi* [40]. Twenty percent of *O. caspius* transmitted the virus from infected hamster to uninfected hamster. For disseminated infections this was 50% [41].

The host-to-vector-to-host transmission was determined in one experiment [43]. Of *O. caspius* feeding on hamsters, 9.7% to 23.1% transmitted the infection to an uninfected hamster [43].

In summary, the probability of transmission from host to *Aedes*, followed by dissemination, is 0.38 and from *Aedes* with disseminated infection to host is 0.70 (see Table 3). The ranges are wide so we used a range of 0.0 to 1.0 in the uncertainty analysis.

For transmission from host to vector, *Cx. pipiens* s.l. disseminated infections were observed in 18%-22% of feedings [40], and in another study 45% [11]. Transmission from vector to hamster was found in 46.2% [37] to 100% [11] for *Cx. pipiens* s.l. Also mechanical transmission to lambs is reported for mosquitoes feeding on viraemic hamsters, but this is considered to play a minor role [26]. In summary, we used a host to *Culex* transmission probability of 0.22, and a *Culex* to host probability of 0.78 (Table 3).

The stable fly *S. calcitrans* infected 16 out of 40 hamsters (40%) up to 24 hours after feeding on viraemic hamsters [26]. This was caused by mechanical transmission only. The probability of transmission to and from the stable fly cannot be determined separately, hence we assume a probability of 0.63 for both values, derived from 0.63*0.63 = 0.4 (Table 3).

Vertical transmission of the virus to *Aedes* mosquito eggs is indicated as a way for RVFV to bridge inter-epidemic periods. This idea is based on the findings in the early 1980's of infected larvae and pupae of *Ae. lineatopennis* in Kenya [44]. Of these field collections, 2 out of 279 emerging females and 1 out of 731 emerging males were infected. This is only 0.7% of females (Table 3) and 0.3% of males. Studies that reproduce these findings under laboratory conditions are unknown to our knowledge.

Table 3. Estimated transmission probabilities and their range (used in the uncertainty analysis). See Equations 1-16.

Parameter	Definition	Value	Range
ζ	Vertical transmission *Aedes vexans*	0.007	(0.00 – 0.015)
β_{Aedes}	Host to *Aedes* species	0.38	(0.00 – 1.00)
β_{Culex}	Host to *Culex* species	0.22	(0.00 – 1.00)
$\beta_{Stomoxys}$	Host to S. calcitrans	0.63	(0.00 – 1.00)
α_{Aedes}	*Aedes* species to host	0.70	(0.00 – 1.00)
α_{Culex}	*Culex* species to host	0.78	(0.00 – 1.00)
$\alpha_{Stomoxys}$	*S. calcitrans* species to host	0.63	(0.00 – 1.00)

Host preference of the vector

Comparison of different baits in traps showed that the bovine-baited net was by far the most effective trap to catch *Aedes vexans*, with 53.6% of all collected *Ae. vexans* mosquitoes in all traps. It was followed by the sheep-baited net (16.7%), man-baited net (12.6%) and chicken-baited net (11.6%) [34]. Field collected mosquitoes in Senegal showed that overall 53.2% of the blood meals from *Ae. vexans* were taken on equine, 18.6% on bovines, 7.1% on sheep and 0.6% on human. No blood meal was taken on rodents [34]. In the United States *Ae. vexans* collected in nature had fed in 80% on mammals, consisting of humans (31%) and white tailed deer (48%) [45]. As no host densities are known in these nature areas, these figures are only indicative for a preference towards mammals, which is confirmed by others [46].

Determining the host preference of *Culex pipiens* s.l. is fraught with uncertainty as this vector is a complex of subspecies, which range from pure ornithophilic to totally opportunistic mosquitoes [46]. The subspecies hybridize, producing populations with intermediate preferences. For example 52% of *Cx. pipiens* s.l. caught in Egyptian villages had fed on humans, 9.8% on cattle and 1.8% on sheep. Only 4.5% had fed on chicken [47]. In the United States, 16% of *Cx. pipiens* s.l. had fed on mammals [45], and in Russia a similar 19% had fed on humans [48].

Table 4 shows the estimates of host preferences as used in the model. They are expressed as relative numbers, of which that for the most preferred host is set to 1.0.

Table 4 Host preferences π_{ij} which determine the probability of vector *i* biting host *j* for host densities N^h_j (see Equation 7).

Vector	Host	Value	Range
Aedes vexans /Aedes cinereus	Cattle	1.0	(0.0 – 1.0)
	Sheep and goat	0.3	(0.0 – 1.0)
	Birds	0.2	(0.0 – 1.0)
Culex pipiens s.l.	Cattle	0.2	(0.0 – 1.0)
	Sheep and goat	0.2	(0.0 – 1.0)
	Birds	1.0	(0.0 – 1.0)
Culex pipiens molestus	Cattle	1.0	(0.0 – 1.0)
	Sheep and goat	1.0	(0.0 – 1.0)
	Birds	1.0	(0.0 – 1.0)
Culex pipiens s.s.	Cattle	0.0	–
	Sheep and goat	0.0	–
	Birds	1.0	–
Stomoxys calcitrans	Cattle	1.0	–
	Sheep and goat	1.0	–
	Birds	0.0	–

2.3.4. Population sizes of hosts and vectors

The abundance of hosts and vectors per 5 x 5 km grid in the Netherlands was acquired from external sources. The abundance of hosts (cattle, sheep, goats) was determined from a database of 'Dienst Regelingen' of the Ministry of Economic Affairs, Agriculture and Innovation (EL&I) and the mosquito abundances, consisting of *Ae. vexans*, *Ae. cinereus* and *Cx. pipiens* s.l., were determined by Avia-GIS [24].

In short, the mosquito abundances by Avia-GIS are mainly based on 1000 sampling points from mosquito traps in Belgium in 2007-2008, which were then extrapolated to the Netherlands using landscape, vegetation, temperature, precipitation and soil data. Mosquito abundances are assumed to be related to these properties, as that represents the availability of breeding sites. Mosquito abundances are assumed to be independent of host densities.

The mosquito abundance is here the yearly maximum number of mosquitoes expected to be caught during a 7 day catch with CO_2 traps. Following the assumptions in [49] we assume that 1% of the total mosquito population present in an area of 1 km^2 is caught by one trap. Multiplication with 2500 will thus result in the number of mosquitoes per 5 by 5 km grid. This crude assumption will be subject of the uncertainty analysis of the model, assuming a 10-fold smaller and larger mosquito abundance.

The abundance of the stable fly *S. calcitrans* is linked to the number of hosts present, because they live very closely to their hosts. The estimate for the *S. calcitrans*-to-cattle ratio is 304.0 (26.8-540.0) based on data from the United States [50-52]. This ratio is calculated assuming that these flies only feed on legs of their hosts, that they feed approximately 30 minutes per bite (one bite per day) and have an active period of 10 hours per day [50].

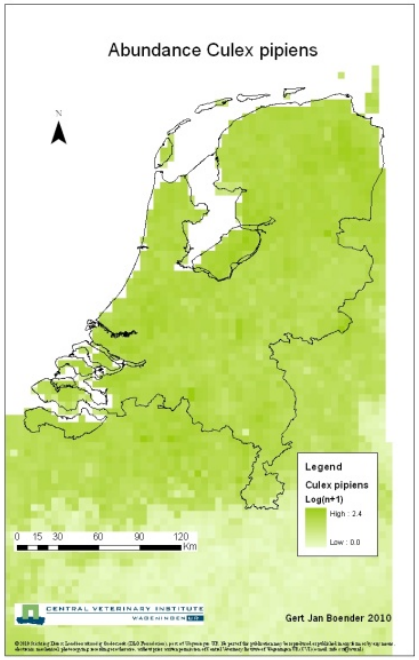

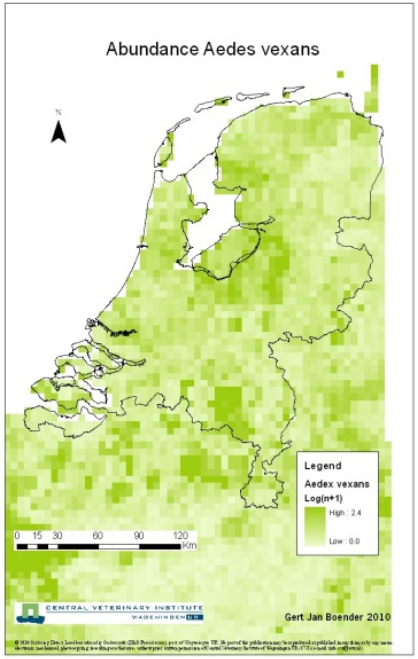

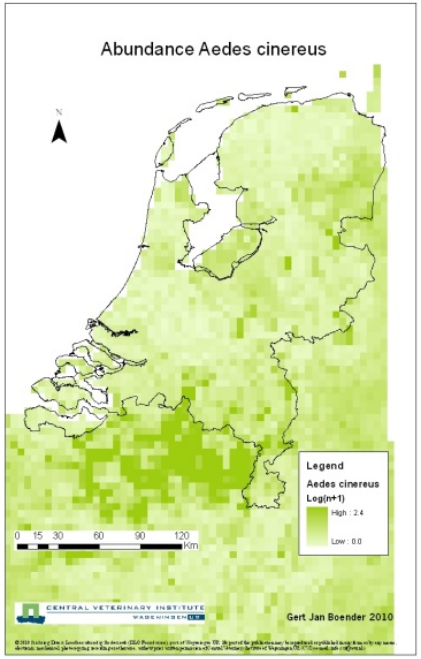

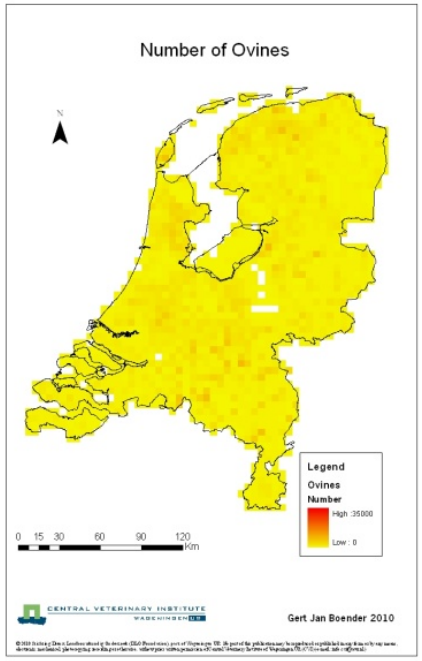

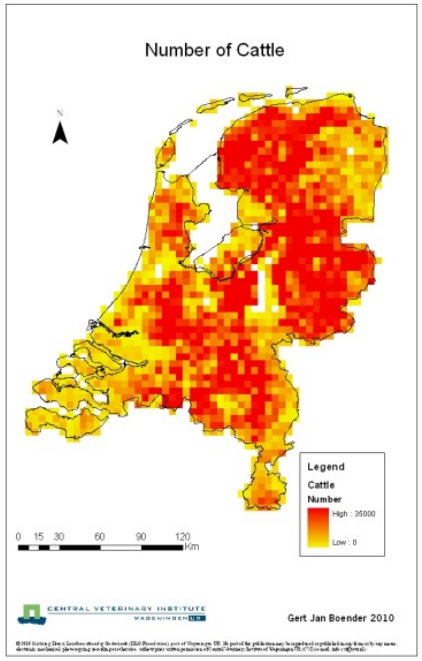

Figure 2. Vector abundance of three mosquito species and host abundance per 5 by 5 km grid cell in the Netherlands.

Seasonality of vector abundance

Based on the temperature threshold for mosquito biting of 9.6 ºC [12] and temperature data of De Bilt in the Netherlands (of 1971-2000, KNMI), it was determined that during an average year the mosquitoes are only active (i.e. biting rate > 0) in the period between 21st of April and 23rd of October. This period is called the vector season. As temperature (24h average) and vector abundances vary during the season, the potential of a RVF outbreak occurring in the country is presented in this report at 3 moments during the vector season: at 30 days after the start of the vector season (21st May), half way (23rd July), and 30 days before the end of the vector season (23rd September).

The temporal changes in mosquito abundances during the year in the Netherlands were estimated from data of Takken et al. [53]. These data comprise of monitoring during July-Oct 2005 and March-July 2006 at different sites in the Netherlands.

CO_2 traps catch female mosquitos looking for a blood meal, which is called aggressiveness [36]. The numbers caught by such a trap are thus the number of females which have fulfilled a gonotropic cycle. As that cycle depends on temperature (and so does the number of bites per time), the mosquito catches in CO_2 traps depend on temperature as well. A simple model correcting for temperature was applied. We assumed that the mosquito population size follows a sinoidal pattern during the vector season with length θ. To derive the maximum population abundance v_{max} and the phase v_a, we used the observed catch data $C(t, T_t)$ and the biting rate $b(T_t)$ as function of daily (24h) average temperature T_t (from literature). Mosquito catches of Takken et al. [53] for which the temperature (24 h average) was lower than 9.6ºC were excluded.

$$C(t, T_t) = b(T_t) \cdot v(t)$$
$$= b(T_t) \cdot \frac{1}{2} v_{\max}\left(1 + \sin(\frac{2\pi \cdot t - v_a}{\theta})\right) \qquad \text{Equation 17}$$

We did not have data to correct for temporal changes of the population size of the stable fly *S. calcitrans* in the Netherlands. The temporal pattern of *S. calcitrans* was constructed assuming a non-growing yearly averaged population size and a mortality rate based on temperature fluctuations [33].

3. Application of the model

3.1. Risk maps

Risk maps are a visualization of a certain risk measure on a geographic map. The maps produced in this report are based on a grid representation of 5 by 5 km areas in the Netherlands. The number of hosts for each grid cell is the sum of all cattle, sheep and goats of the farms located in that grid cell. The host abundance and vector abundance and the estimates of the other 24 parameter values of the model determine the outcome of the model, i.e. the value of the risk measure in that 5 by 5 km area (see Figure 3).

For each 5 by 5 km grid cell, vector abundance for each mosquito species is determined by geographical and climatological features by Avia-Gis [24], and the host abundance (cattle, sheep and goats) is obtained from a database of 'Dienst Regelingen' of the Ministry of EL&I (see Figure 3).

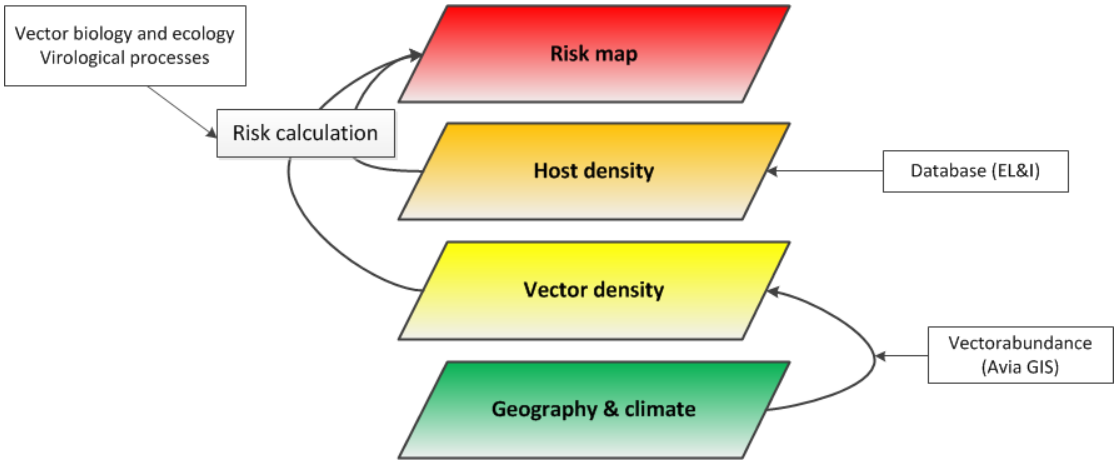

Figure 3. Procedure followed during the creation of a risk map. The data for vector abundance are acquired from Avia-GIS [24] and for host abundance from the Ministry of Economic affairs, Agriculture and Innovation (EL&I).

Two types of risk maps will be distinguished in this section. A map depicting (1) the risk of persistence of RVF and (2) the risk of an outbreak of RVF. An infection can only persist when the long term average epidemic growth rate in that area is larger than the threshold value 0. This long term average is calculated by a Floquet multiplier for which the algorithm is given in Appendix I.

Although a long term epidemic growth rate smaller than the threshold of 0 indicates that the infection cannot persist, it does not mean that the growth rate at a certain moment during the year is never larger than 0. When that growth rate is larger than the threshold 0, an outbreak can occur at that time.

The *probability* for each of the 5 by 5 km areas to have a long term epidemic growth rate larger than the threshold value 0, is determined by the reference curve as described in section 22. The same is done for the growth rate at a certain moment. In short, the risk of persistence or of an outbreak is determined by the fraction of model outcomes (after sampling parameter values) being an epidemic growth rate larger than 0, for a given host and vector abundance.

3.2. Uncertainty analysis

None of the parameter values of models can ever be determined with exact precision. An uncertainty analysis helps to identify the parameters for which the uncertainty of the parameter estimate has the largest impact on the outcome of the model. In an uncertainty analysis, the model is used with parameter values each ranging within their biological plausible interval. Its outcomes reflect the magnitude of uncertainty introduced in the model outcome by the uncertainty in parameter estimates. This differs from a sensitivity analysis, that only shows the change in outcomes by changing a parameter value, even if this is biological implausible.

An uncertainty analysis determines the range and distribution of possible outcomes given the uncertainty in parameter values. The RVF model has 24 parameters (without considering the stable fly *S. calcitrans*) and systematically changing all parameter values would result in too many outcomes and calculations. Latin hypercube sampling reduces the number of outcomes to be computed with still a good coverage of the parameter space. This method involves a structured sampling scheme based on the distribution of parameter values describing the parameter uncertainty. Parameter values that were estimated with a high level of accuracy have a narrow distribution around the point estimate, whereas very uncertain parameters have a large range. The ranges used in the uncertainty analysis are given in Table 1, Table 2 and Table 3.

The host and vector population sizes are varied in the uncertainty analysis by randomly selecting 50 areas of 5 x 5 km (each area representing a host and vector population). Additionally, mosquito abundance is changed 10 fold (smaller or larger, see 2.3.4) using an extra parameter.

The correlation between outcome of the model (here initial epidemic growth rate after introduction of RVFV) and each of the sampled parameter value is determined by the Kendall rank correlation coefficient (KRC). KRC is a non-parametric measure of correlation, such that the magnitude of the parameter does not determine the outcomes of the uncertainty analysis. KRC coefficients of -1 or 1 represent a perfect correlation of outcome with parameter, correlation of 0 means no correlation. So the higher the (absolute value of) KRC, the more important that parameter is for the outcome of the model. Thus, such parameters are very important and the others are not or less, helping us with selecting future experimental work. To determine whether a KRC coefficient is different from 0, 100 dummy variables were used in the uncertainty analysis to determine the 5% confidence interval of the KRC coefficient.

Reference curve

The results of the uncertainty analysis can also be used to determine the *probability* of an area in the country being at risk of a RVF outbreak, i.e. the probability that the initial epidemic growth rate is higher than 0. For each 5 by 5 km area we can calculate the point estimate of the epidemic growth rate (at a certain moment in the year) by using the point estimates of the 24 parameters as input, but the uncertainty analysis yields a distribution of growth rates for each area, and a certain fraction of these growth rates is higher than 0. To save computer time, we did this for 50 randomly chosen areas (differing in vector and host abundance), and subsequently constructed a reference curve. This curve determines the probability of the epidemic growth rate being larger than 0, as a function of its point estimate (i.e. the outcome of the model with the default parameter values).

These values were plotted as a reference curve and this curve was used to create maps showing the probability of an outbreak in each 5 by 5 km area in the country (epidemic growth rate being larger than 0). The same reference curve was used to create maps showing this for the long term average growth rate during the year, i.e. for persistence of RVF in each 5 by 5 km area.

3.3. Control measures: vaccination, culling and vector control

3.3.1. Vaccination

Vaccination of livestock can be used to control RVF by prevention of an outbreak. For the assessment of the vaccination effect, we will consider a 'perfect' vaccine. A perfect vaccine is defined here as a vaccine that prevents animals of *becoming infectious*. The model includes vaccination by creation of a new state of the host animals being vaccinated and immediately fully protected. These animals will not be infected and thus will not transmit the infection. In this way, the effect of vaccination before introduction of RVFV in the country will be studied, on both the outbreak and on the persistence of the infection. Emergency vaccination during a RVF outbreak is not studied here.

Vaccination with a perfect vaccine decreases the number of susceptible animals and adds vaccinated hosts to the population that will be bitten by infectious mosquitoes without producing viraemic hosts. The minimal fraction of animals to be immunized by a perfect vaccine for the prevention of an outbreak or for prevention of persistence of the infection is the critical vaccination degree. This is the threshold at which the (long term) epidemic growth rate is 0.

3.3.2. Culling

The control by culling of animals is investigated for on-going outbreaks, because culling is an intervention used in a crisis situation. After the start of an outbreak (here: in a 5 by 5 km area), it will take a certain time delay before the infection will be detected for the first time in that area. Therefore, culling will be studied by simulation of outbreaks with detection delays of 0, 10, 30 and 60 days after introduction of RVFV in the 5 x 5 km area. After these delays animals will be culled with a rate of 1 day^{-1}, meaning that animals are culled on average after 1 day. With this 'idealistic' scenario the effect of immediate cull of hosts after detection of the infection will be studied. Two culling strategies are taken into account: (1) culling only seropositive animals (with a perfect diagnostic test) and (2) culling of all animals. The strategies are compared with the epidemics without control.

For RVF it is only feasible (in practice) to distinguish between serological positive and negative animals, and not between viraemic and non-viraemic animals. Seroconversion occurs somewhere during the infectious period, and animals remain seropositive after recovery. For example, for mice the first serological positive test was at day 4, while virus could be detected by PCR up to day 8 [54]. Future experiments might provide more information on the seroconversion of mammals other than mice. We chose for seroconversion half-way during the infectious period. Hence, culling of seropositive animals includes culling of both infectious and recovered (immune) animals in the model.

3.3.3. Vector control

Vector control can be applied during an outbreak and previous to an outbreak when the RVF threat is high. Vector control is modelled as a reduction in the vector population abundance. Prolonged reductions in vector populations can best be done by larval control, for instance using *Bacillus thuringiensis*. In crisis situations a reduction of the adult population by adulticides can be maintained for a while. Both methods result in a reduction of the abundance of vectors. Here, we calculate the reduction in vector population needed to prevent outbreaks and to prevent persistence of infection, in the most favourable season (July).

3.4. *Stomoxys calcitrans* and *Anopheles macullipennis*

3.4.1. *Stomoxys calcitrans*

Although evidence is scarce for the role of the stable fly *S. calcitrans* in the RVF epidemics in Africa and only one study reports its competence [26], it is a potential vector for RVFV. The stable fly is abundant and the vector capacity among hamsters is high [26], therefore we chose to study this potential mechanical vector.

We will investigate the critical vector-host ratio (and not the vector abundance), because unlike for mosquitos the abundance of the stable fly is mainly determined by host density [50-52] and not by other aspects (vegetation) of the area in the country. Therefore, we exclude the use of risk maps here. Persistence and outbreaks are studied here (as in the whole report) in 5 by 5 km areas, without hosts being subdivided into separate herds. Thus, we assume that stable flies can move easily from herd to herd within a 5 by 5 km area.

3.4.2. Anopheles macullipennis

Members of the *An. macullipennis* complex were vector of indigenous malaria in the Netherlands until the beginning of the 20th century [55]. *An. macullipennis* s.l. females were found in sheep stables in a study in 2010 (pers. comm. E.J. Scholte). The competence of this species complex to transmit RVF was never tested. The abundance of this species was estimated by AviaGIS [24].We will create risk maps for this species assuming they have the same parameter values as *Cx. pipiens* s.l or as *Ae. vexans*.

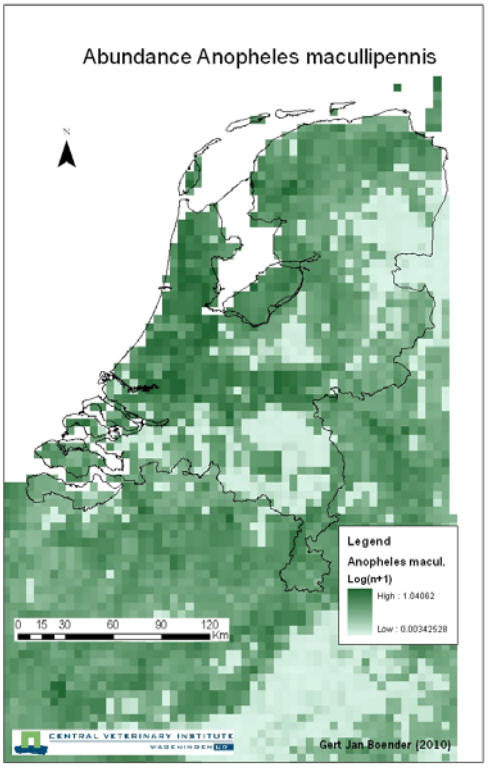

Figure 4. Vector abundance of the *An. macullipennis* complex per 5 by 5 km grid cell in the Netherlands.

3.5. Nature reserve 'De Oostvaardersplassen'

Investigation of the role of nature reserves for the risk of an RVF outbreak in the Netherlands is done for the 'De Oostvaardersplassen'. This is a wetland area with heck cattle, konik horses and red deer in the province Flevoland.

Horses are not hosts for RVFV. Furthermore we consider three possibilities, because susceptibility to RVFV of deer and preference of vectors for deer are unknown: (1) deer is a competent host for RVFV equivalent to cattle, and vector species have an equal preference for cattle and deer, (2) deer is not a competent host, and vector species have an equal preference for cattle and deer, and (3) deer is not a competent host, but also not preferred (not bitten) by the vector species.

4. Results

4.1. Risk maps

4.1.1. Persistence (long term epidemic growth rate)

The map for risk of persistence of RVFV (after accidental introduction) in the Netherlands is presented in Figure 5. This map shows that both high risk and low risk areas for persistence exist, according to the model. Interestingly, the areas with a high host abundance (see Figure 2) have the lowest risk of a persistent RVF infection, due to a 'dilution effect of infected hosts' which we will explain in the Discussion. Furthermore, the risk of a persistent infection is high in nature reserve areas, which is partially due to the fact that wildlife (free range cattle and deer) was not included as host to create this risk map, but only domestic livestock. Results for the nature reserve 'Oostvaardersplassen' is shown later (see 3.5).

The importance of the different mosquito species in the risk of persistence is shown by calculations with each of the vector species separately (Figure 6). Comparing the map for *Cx. pipiens* s.l. (Figure 7) with Figure 6 (including all mosquito vector species) shows clear similarities, while the low abundance of *Aedes* species in the Netherlands results in almost no risk.

The mosquito abundances as used in the model are highly uncertain due to the uncertain step from mosquito trap catch to population abundance in the whole 5 by 5 km area. Therefore, two additional risk maps were created with a 10 fold lower and a 10 fold higher population abundance of the vectors. Figure 7 shows that this 10 fold difference in vector population size dominates the results of the risk map.

4.1.2. Outbreaks (epidemic growth rate at a certain time in the year)

The risk of outbreaks is clearly higher halfway and around the end of the season than at the beginning of the season (Figure 9). This is caused by differences in vector abundances (as observed in trap caches) and by differences in temperature (affecting some model parameters of the vector, see Table 2). Autumn is a risk period for outbreaks as well, although these outbreaks will be short by the decline in mosquito abundance later in autumn/winter.

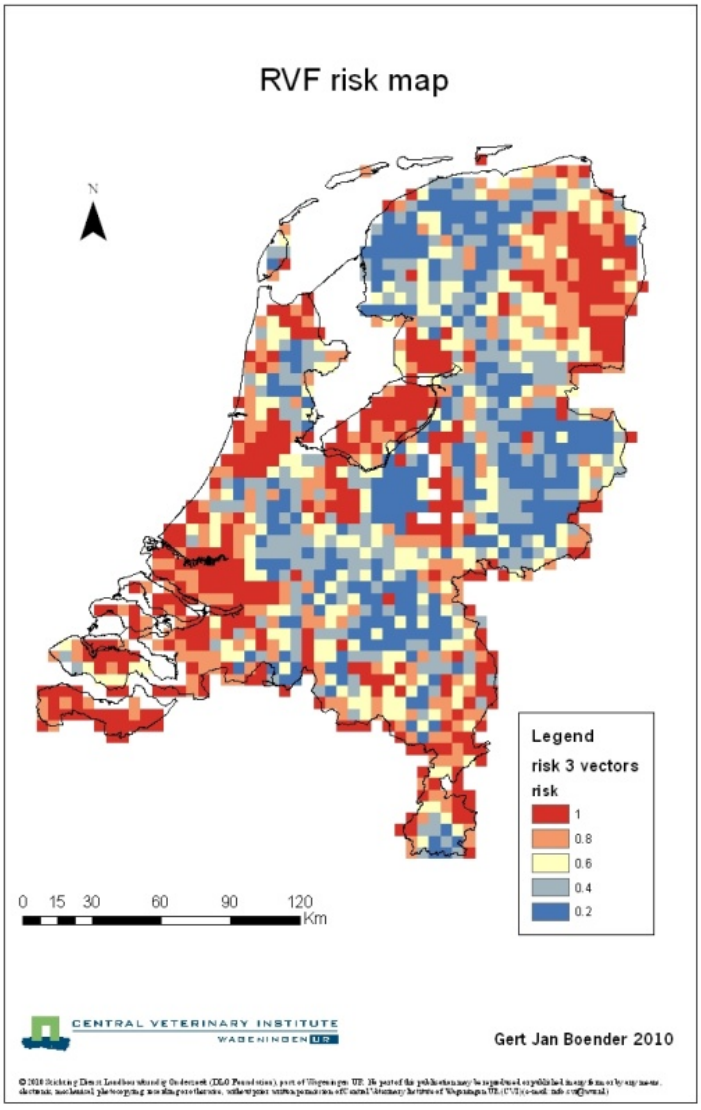

Figure 5. Risk of persistence of RVFV in the Netherlands. Blue indicates a low probability (<20%) of the long term epidemic growth rate exceeding the threshold of 0, and red indicates a high probability (>80%).

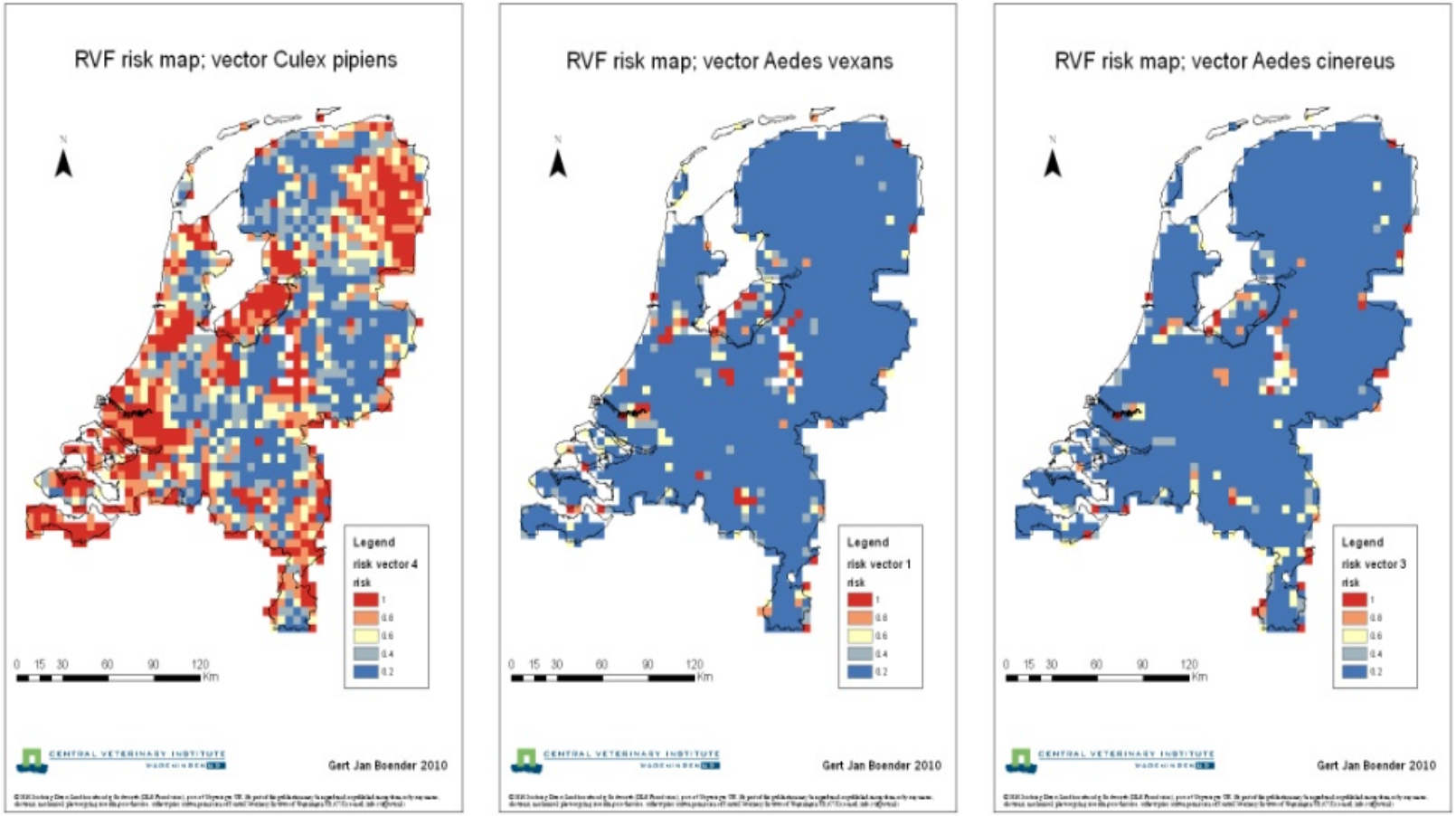

Figure 6. Risk of persistence of RVFV in the Netherlands if the indicated vector is the only competent RVFV vector in the country. Blue indicates a low probability (<20%) of a long term epidemic growth rate exceeding the threshold of 0 and red indicates a high probability (>80%).

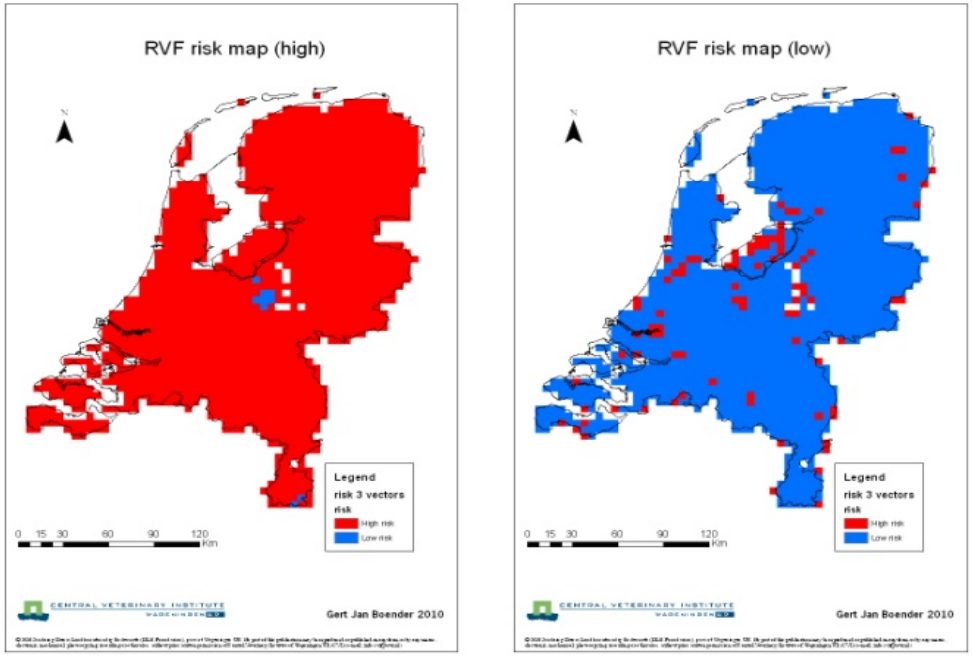

Figure 7. Areas with long term epidemic growth rate higher than the threshold of 0 (red) and lower (blue) for vector population sizes 10 fold higher (left) and 10 fold smaller (right)

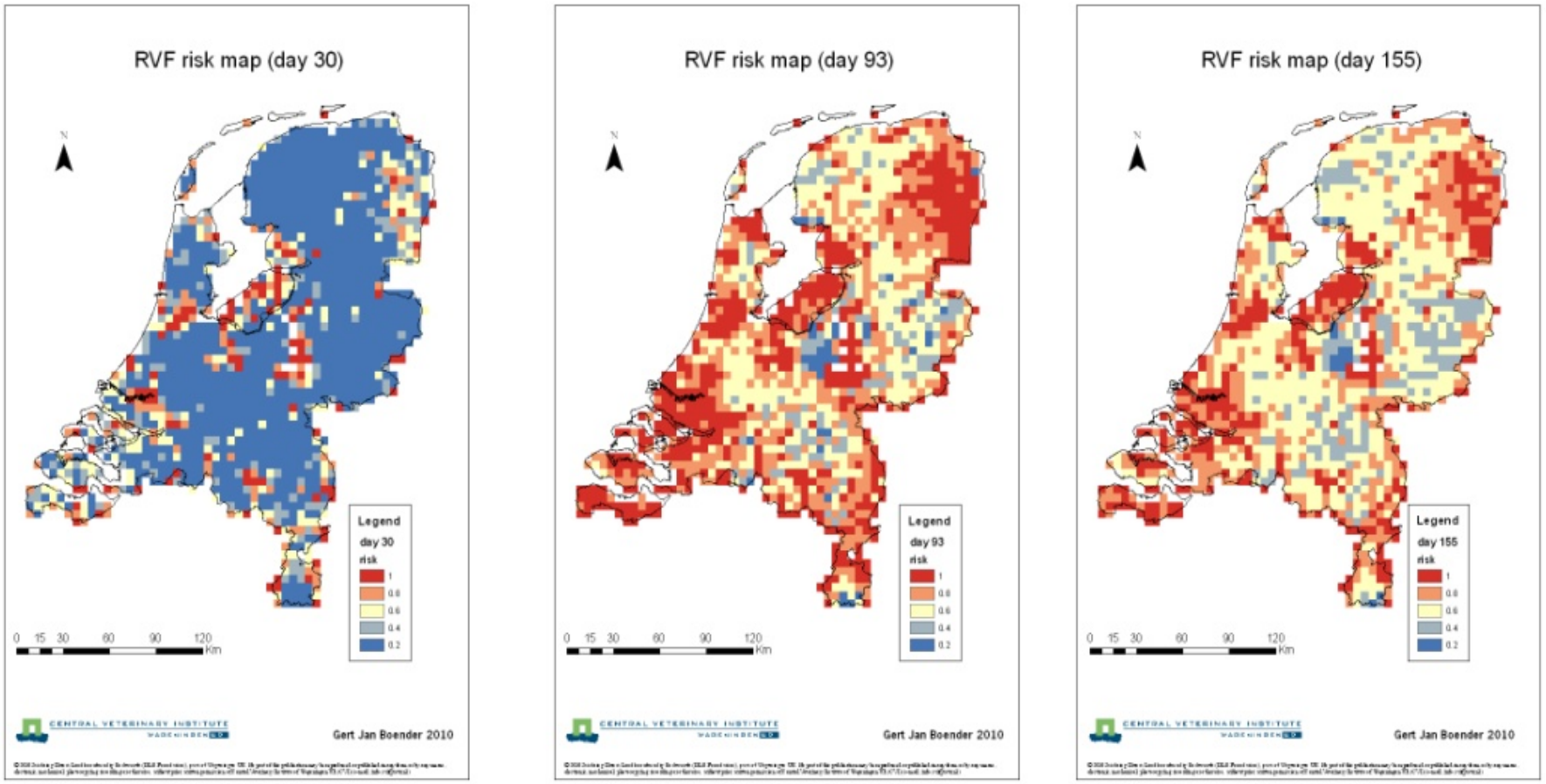

Figure 8. Risk of RVF outbreaks in May, July and September. Blue indicates a low probability (<20%) of the initial epidemic growth rate exceeding the threshold of 0 and red indicates a high probability (>80%). Day 1 (21 April) is the beginning of the season in which mosquitos are active.

4.2. Uncertainty analysis of the mathematical model

Using the Kendall Rank Correlation test, the correlation between output and each model parameter was calculated (Figure 9). Parameters in the figure are ordered by their absolute KRC value. The most important parameter for the model outcome is the vector-host ratio, due to the high level of uncertainty and variation in the vector abundance. Also parameters associated with the extrinsic incubation period in the mosquito are of importance.

Interestingly, the relationship of biting rate of the vector with temperature does not have a large effect on the model outcome, which is caused by the small range around the point estimate of the biting rate, as observed and taken in the uncertainty analysis.

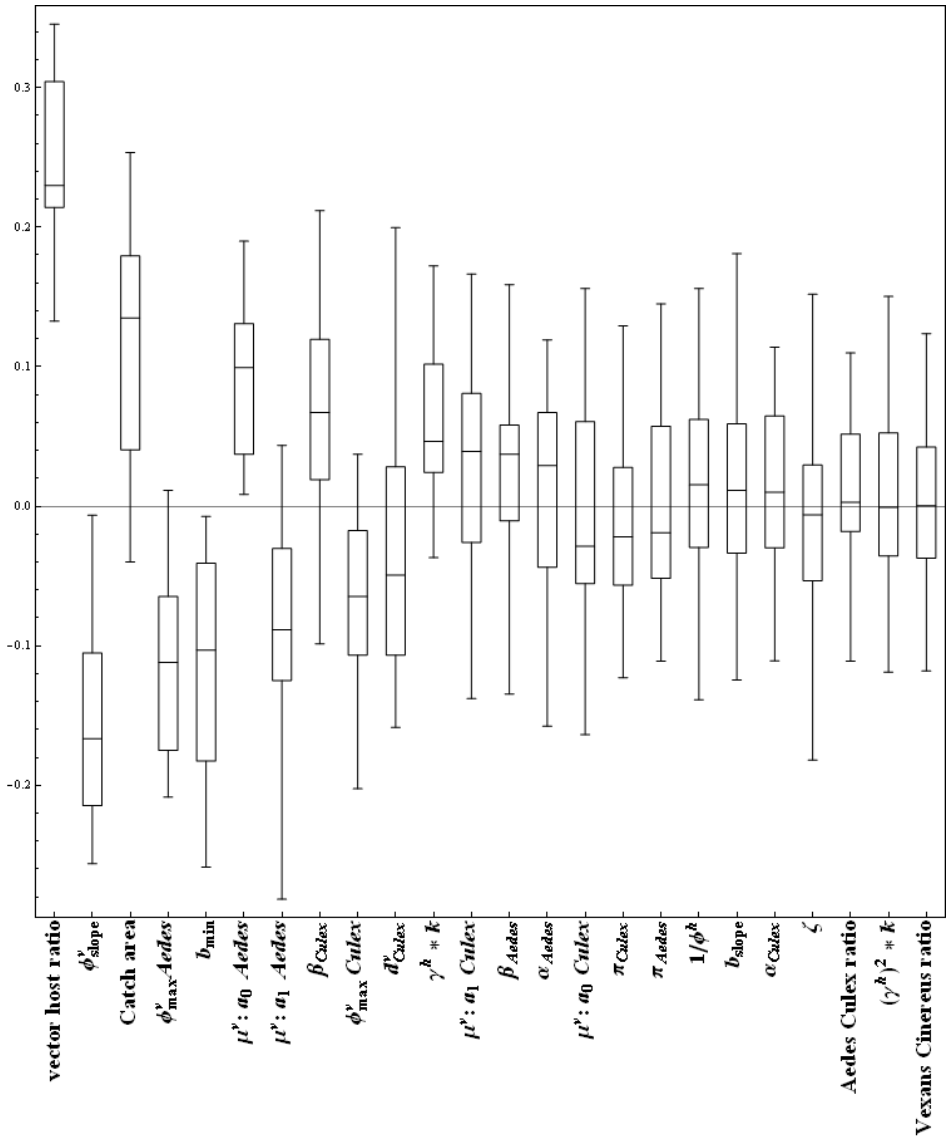

Figure 9. Kendall Rank Correlation coefficients for 24 parameters in the uncertainty analysis. Parameters are orderd by their absolute KRC value. For the explanation of parameters, see Tables 1-4.

Reference curve
The curve in Figure 10 describes the probability that the epidemic growth rate is larger than 0 (y-axis), as function of the point estimate of the epidemic growth rate (x-axis, calculated with the point estimates of each parameter value). This reference curve was subsequently used to determine the *probability* of persistence or of an outbreak for all 5 by 5 km areas in the risk maps.

Most dots in Figure 5 are characterized by negative X-axis values, i.e. most (70%) of the 50 randomly selected areas are characterized by an epidemic growth rate below the threshold of 0, when using the default (point estimate) parameter values. However, for these areas the probability that the 'actual' epidemic growth rate is larger than 0, is not 0 but ranges from 0.06 to 0.42.

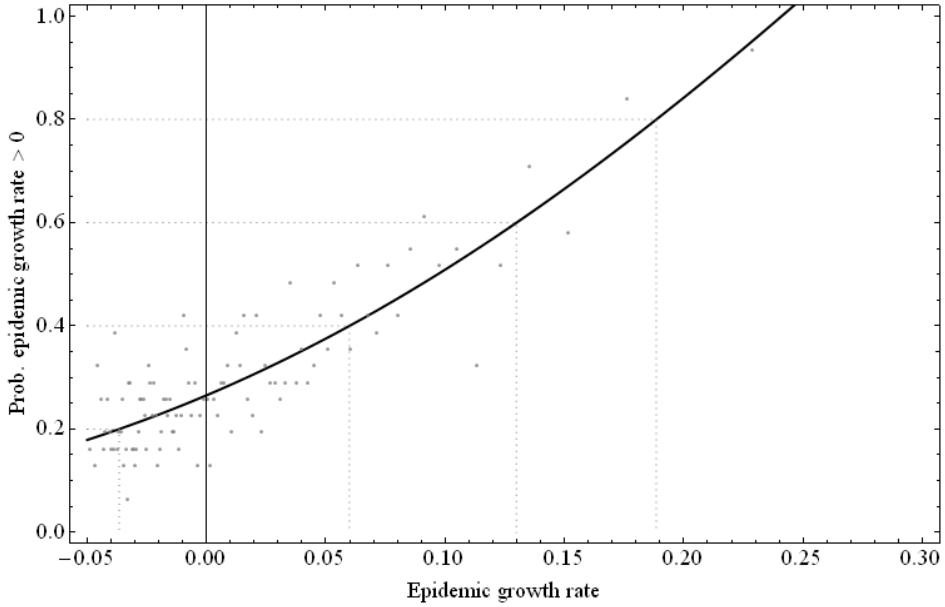

Figure 10. Reference curve, showing the probability of the epidemic growth rate (at a certain time in the year) to be higher than 0, for different values of the point estimate of epidemic growth rate (calculated with the default parameter values).

4.3. Effect of control measures

Two livestock areas of interest were chosen to study the impact of control measures: a densely populated livestock area (DPLA) in the province of Gelderland and a sparsely populated livestock area (SPLA) in the province of South-Holland. The characteristics of these areas are given in Table 5, together with their long term epidemic growth rate of RVF.

Table 5. Characteristics of the two chosen areas in the Netherlands to evaluate control measures. Vector-host ratios are 190 in the SPLA and 2.6 in the DPLA.

Area	Cattle	Sheep & goat	*Ae. vexans*	*Ae. cinereus*	*Cx. pipiens*	Long term epidemic growth rate
	per 5x5 km					
SPLA	125	75	3100	2550	32,500	0.20
DPLA	11,625	2875	3100	2550	32,500	-0.04

SPLA = sparsely populated livestock area; DPLA = densely populated livestock area

4.3.1. Outbreaks without control

The long term epidemic growth rates calculated with the default parameter values is 0.20 for the SPLA and -0.04 for the DPLA. The simulated outbreaks at different moments during the season, starting with one latently infected bovine host, are shown in Figure 11.

The largest outbreaks occur with introduction of the infection in the middle of the summer (July). Circumstances for spread of the infection, like vector abundance and temperature, are most favourable at that moment. The number of infected hosts shows a sharp increase and decreases again to low numbers within a relative short period (approximately 20-30 days). The infected vector population lags behind, shows a slower increase but remains present during a much longer period (approximately 70-80 days). In an SPLA with only 200 hosts per 5 by 5 km (and thus a high vector-host ratio of 190), the peak can be as high as 20% of the vectors being infected.

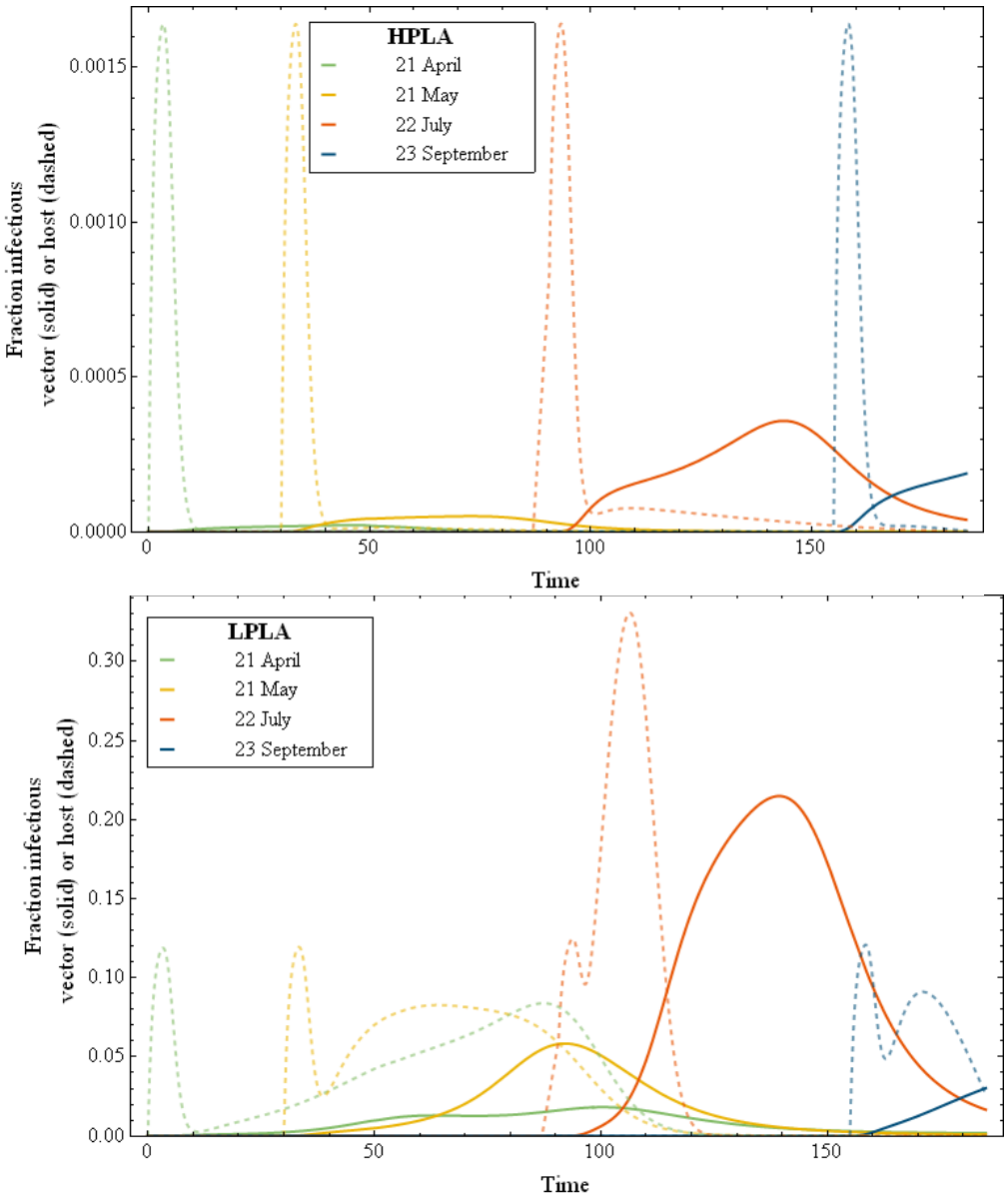

Figure 11. Simulated outbreaks for RVFV introduction at 21 april, 21 may, 22 july and 23 september in a sparsely populated livestock area (upper) and a densely populated livestock area (lower). Infected vectors are shown with solid lines and infected livestock by dashed lines.

4.3.2. Culling

Culling was studied using simulations of outbreaks in an SPLA, so in an area with a high vector-host ratio, with a detection delay of 0, 10, 30 or 60 days. Two culling strategies were taken into account: (1) culling only seropositive animals and (2) culling of all animals. Culling of all animals is studied here to look at the results from a theoretical point of view. In practice when all hosts within an area are culled in a few days, the outbreak stops at the same time in that area. However, if only a few farms are completely culled in an area and vectors fly to the farms that are not culled, this scenario becomes more realistic.

A RVF outbreak starting in July will, without intervention, peaks after 16 days and will be over in 30 days (Figure 11, upper). With a detection delay of 10 days or more, culling of hosts, either all or only seropositive animals, will not affect the

course of the outbreak (data not shown). This is simply due to the fact that the outbreak is either ended by itself (at delays of 30 or 60 days), or because the outbreak peaks already very closely to the start of culling at a delay of 10 days, which makes the impact of culling very small. So culling does not have much effect on the outbreak, when the epidemic growth rate is high like in July. Under these circumstances, culling is always too late, even at a short detection delay of 10 days.

Culling can be effective in other periods of the season, like in periods less favourable for transmission of the virus. Culling of hosts at earlier outbreaks during the season (e.g. starting 21 May) does alter the outbreak (Figure 11). According to the model, at any culling intervention (either culling of all animals or of seropositives only), all animals are either culled or recovered from infection (and thus seropositive) in the end. Therefore, culling has no effect on number of animals lost after an outbreak. The duration of the outbreak is, however, reduced by culling. Both culling of all animals and of only seropositives will shorten the outbreak by weeks, compared to the duration of ca. 130 days without culling (of an outbreak starting on 21 May, see Figure 11).

The fraction of hosts being infectious depends on the choice of which animals will be culled. If only seropositive animals are culled, the peak of fraction infectious animals will increase above the situation without culling (Figure 11, lower). With culling of all animals, the fraction of infectious animals will decrease steeply without showing a higher peak (Figure 12, upper). Of course, the absolute number of animals in the area is then very low.

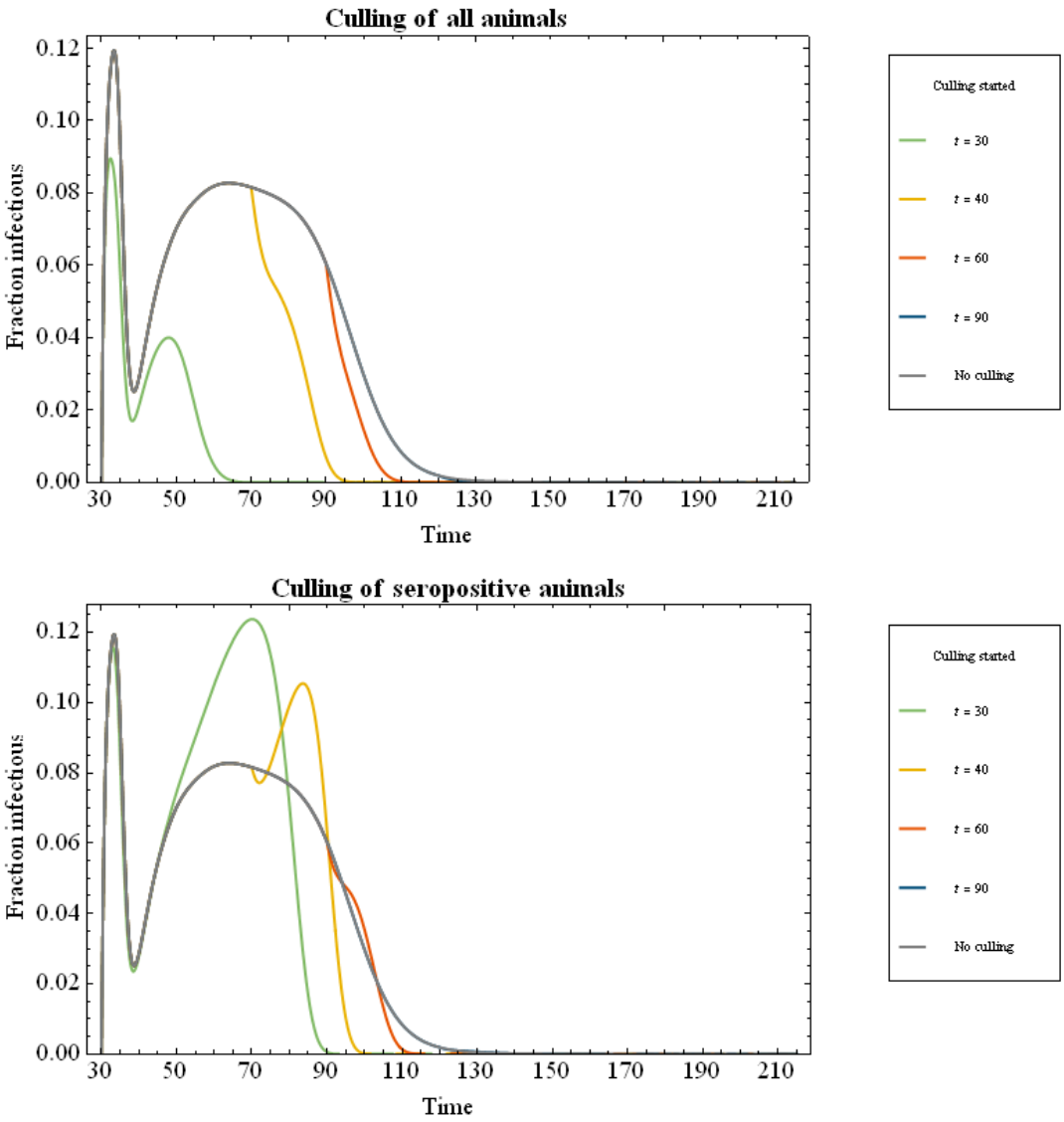

Figure 12. Effect of culling on fraction of infectious animals. The infection is introduced on 21 May (time = 30) and culling starts at time t = 30, 40, 60 and 90 (so with a delay of 0, 10, 30 or 60 days). Culling of all animals is studied here to look at the results from a theoretical point of view. The absolute number of animals in the area is then very low.

Culling increases the maximum fraction of infectious vectors (Figure 13). This explains the acceleration of the outbreak, which shortens the outbreak duration without changing the number of recovered animals at the end. The peak in the fraction of infectious vectors might even be twice as high as without culling.

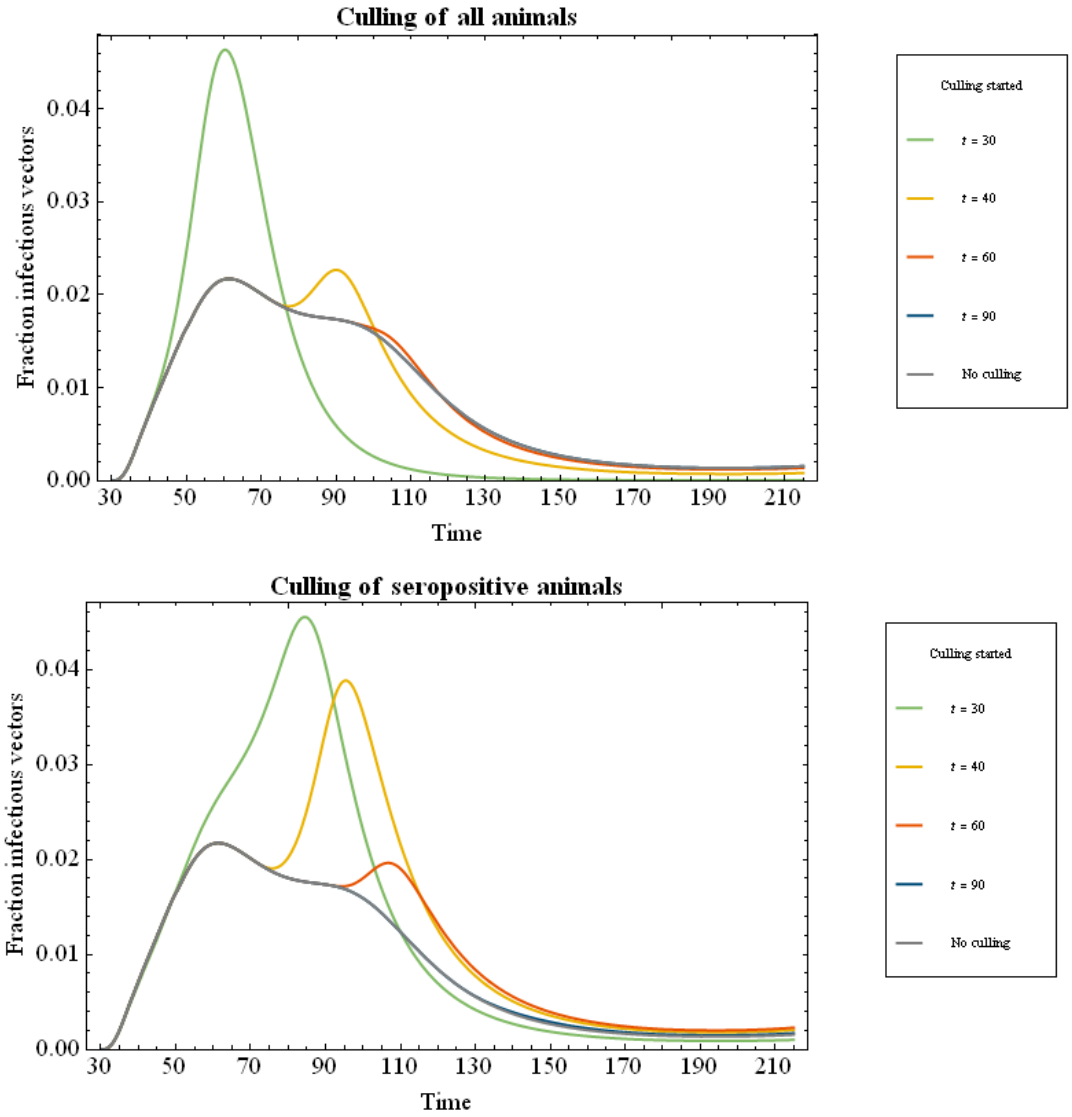

Figure 13. Effect of culling on the fraction of infectious vectors. The infection is introduced on 21 May (time 30) and culling starts at time t = 30, 40, 60 and 90 (so with a delay of 0, 10, 30 or 60 days).

4.3.3. Vaccination

Vector control is modelled as a reduction in vector abundance. The critical vaccination degree to prevent persistence (i.e. long term epidemic growth < 0) is approximately equal to that to prevent an outbreak in the middle and end of the season (July and September, see Figure 13). At the beginning of the season (t_0 = 0, in April) the epidemic growth rate is already smaller than 0 for the range of vector-host ratios of 0-250, so the critical vaccination degree is then 0. For outbreaks starting in May (t_0=30 days) the critical vaccination degree is slightly lower for high vector-host ratios and considerably lower for vector-host ratios below 100 (Figure 13).

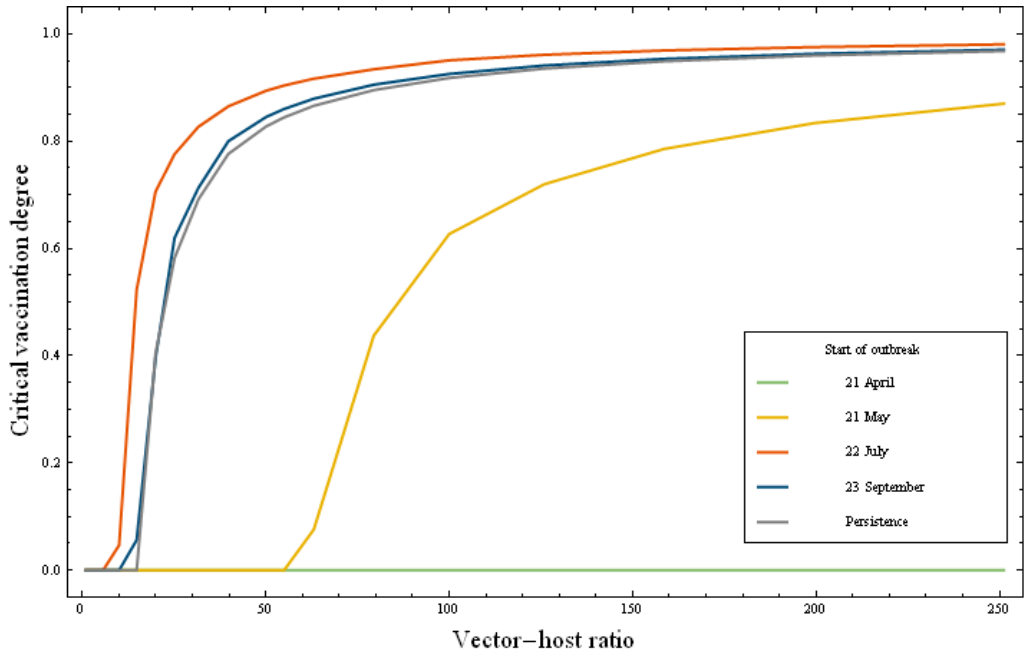

Figure 14. Critical vaccination degree as a function of vector-host ratio for persistence and for an outbreak at 4 moments of introduction of the infection.

4.3.4. Vector control

Vector control was investigated as a method to prevent (new) outbreaks and to prevent persistence in an area. Vector control, for instance by the use of larvicides, reduces the epidemic growth rate of an outbreak (blue lines in Figure 15) and the long term epidemic growth rate (green lines in Figure 15). For a high vector-host ratio such as in an SPLA, a strong reduction of more than 90% of the vector population is needed to obtain prevention of an outbreak and of persistence, by vector control alone (Figure 15 upper). If the vector population is a ten-fold larger, almost all vectors need to be eradicated (Figure 14 upper; upper line). However, the epidemic growth rate then shows a steep decline with reduction in vector population, which might enhance the effect of other control measures.

For areas with a lower vector-host ratio, such as in DPLAs, an outbreak and persistence can even be controlled in the worst-case scenario with a reduction of 40-60% of the vector population (Figure 14 lower; upper lines).

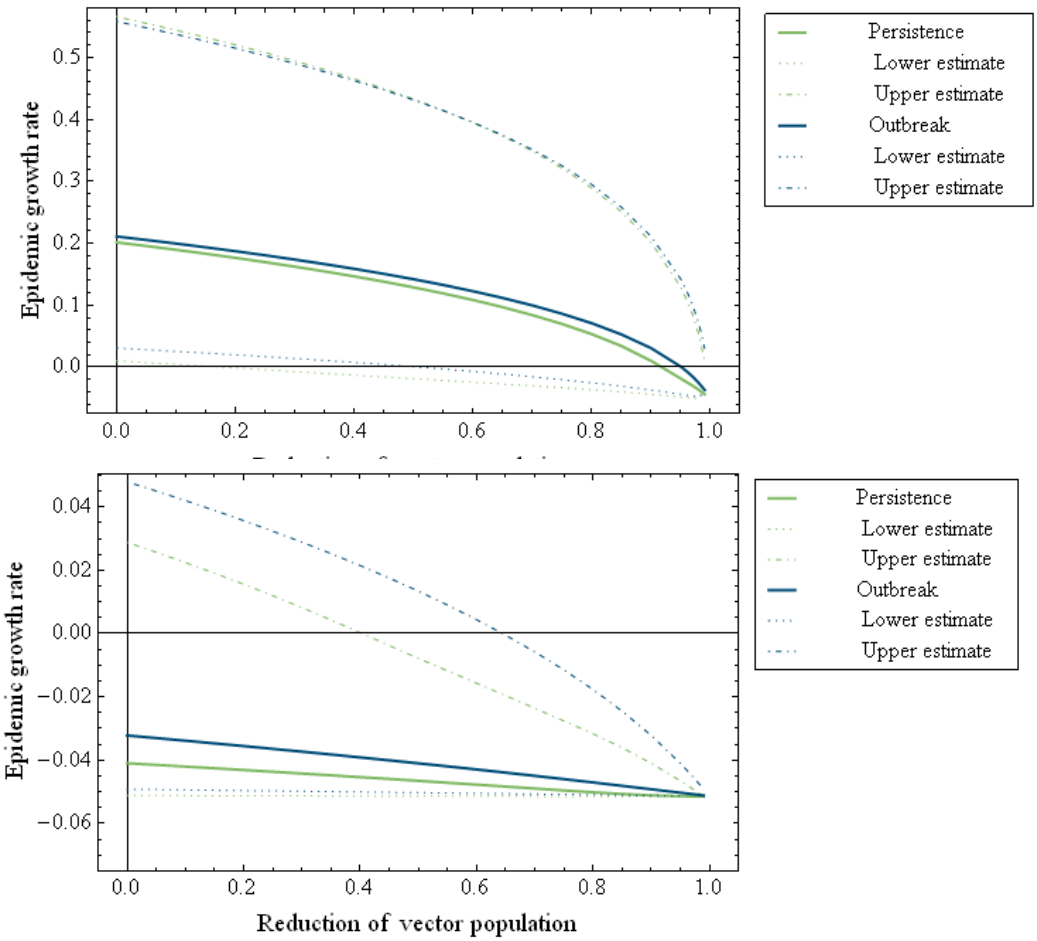

Figure 15. Effects of vector control on the epidemic growth rate and the long term epidemic growth rate for a sparsely population livestock area (upper) and a densely populated livestock area (lower). The mean estimates are given by thick lines; a ten-fold smaller or ten-fold larger initial vector population is indicated by dotted and dotted-dashed lines.The point at which the lines cross the x-axis is the critical vector control threshold for which the (long term) epidemic growth rate drops below 0. The mean estimates for the densely population livestock area (lower) are below the threshold 0 for no vector control.

4.4. *Stomoxys calcitrans* and *Anopheles macullipennis*

4.4.1. *Stomoxys calcitrans*

Persistence

The vector-host ratio of stable flies is taken from several studies in North America [50-52] to be 300 flies per cow, with a wide confidence interval of 27-540. As these numbers can be different for the Netherlands, we studied the relationship between the long term epidemic growth rate and vector-host ratio (Figure 16). The critical value is the vector-host ratio for which the long term epidemic growth rate is equal to zero. i.e. the threshold between persistence and non-persistence. According to Figure 15, already with an extremely low stable fly - host ratio of 1.21 the infection can persist in the area.

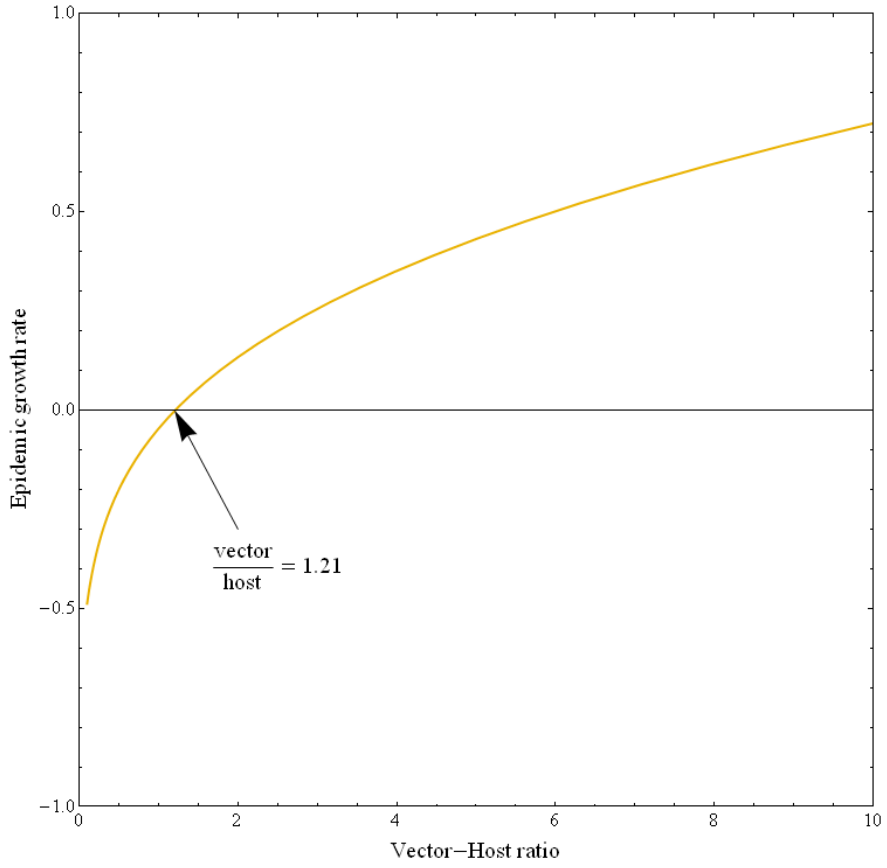

Figure 16. Relation between vector-host ratio and long term epidemic growth rate for the stable fly *Stomoxys calcitrans* in the absence of other vectors. The arrow indicates the critical vector-host ratio.

Persistence of the infection occurs already with very low vector-host ratios, partially due to the high biting rate of stable flies (i.e. at least once a day) and the high transmission probability from vector to host and vice versa (0.63). Another part of the explanation is the fact that the abundance of the flies changes only little during the year (as derived using mortality data [33]) as stable flies are living inside stables.

Outbreaks

To study outbreaks, deterministic simulations were performed in which the stable fly was the only vector. These simulations show (Figure 17) that almost all animals become infected (and thus become seroconverted) when the vector-host ratio is within the expected range (27-540). For lower values the outbreak is slower and fewer animals become infected. During an outbreak up to 20% of the stable flies can be infected when the vector-host ratio is within the expected range (27-540) (Figure 17 lower). However, whether these infected flies can be found during an entomological surveillance depends on the time between collection of vectors and virus detection, due to denaturation of the virus. The half life time of the virus in aerosols is only 6 hours [56].

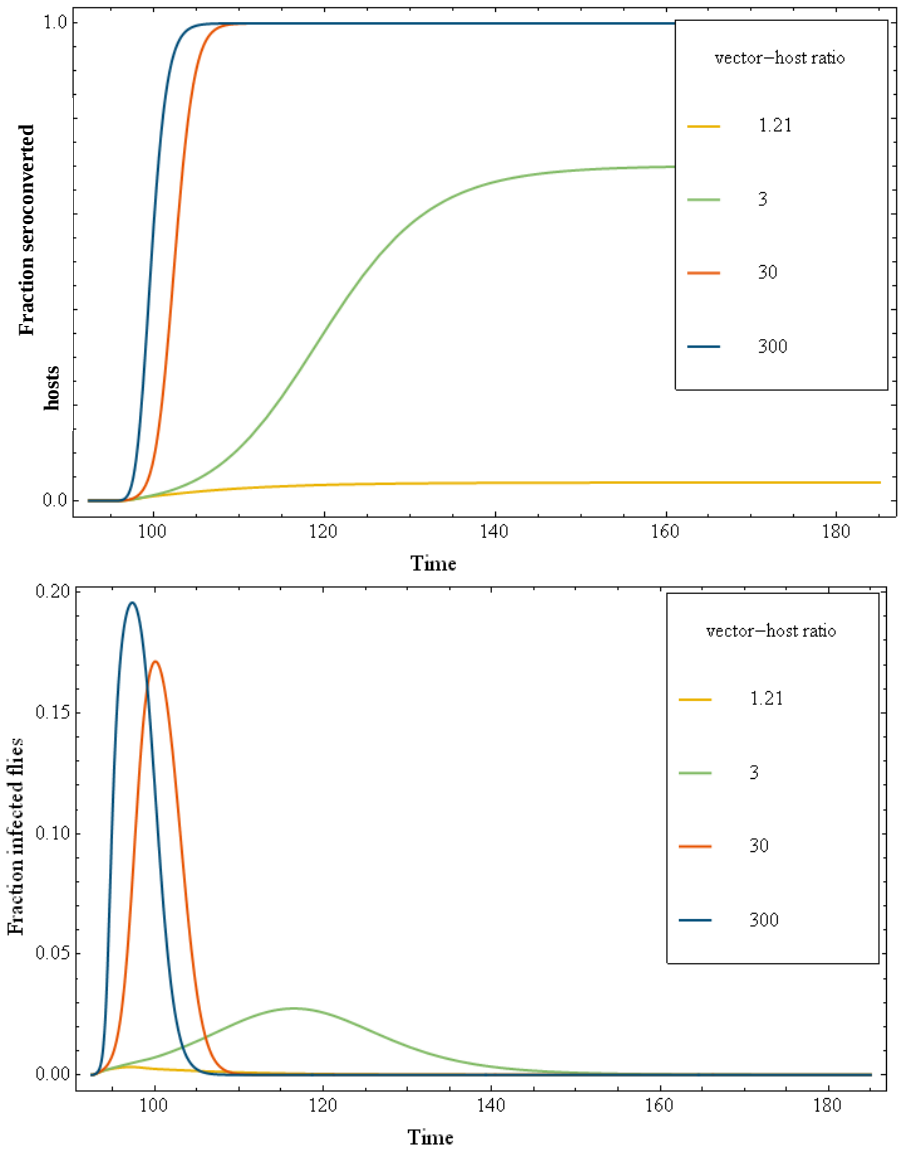

Figure 17. Upper: Fraction of animals that is seroconverted during an outbreak, for the critical (1.21) and higher vector-host ratios. The outbreak started on 22 July (t_0=92.5). Lower: Fraction of infected flies during an outbreak, for the critical (1.21) or higher vector-host ratios. The outbreak started on 22 July (t_0=92.5)

The period during the year in which RVFV is introduced in an area is also of importance for the course of the outbreak. Simulations were performed with a yearly mean vector-host ratio of 30 and starting at the first day of the vector season (21st April), 30 days into the season (21st May), mid-season (22nd July) and 30 days before the end of the season (23rd September). The most rapid growth resulting in the highest peak of infected flies and livestock is found at the end of the season, in September (Figure 18), because the estimated stable fly population size is largest at the end of the season (dotted gray line in Figure 18).

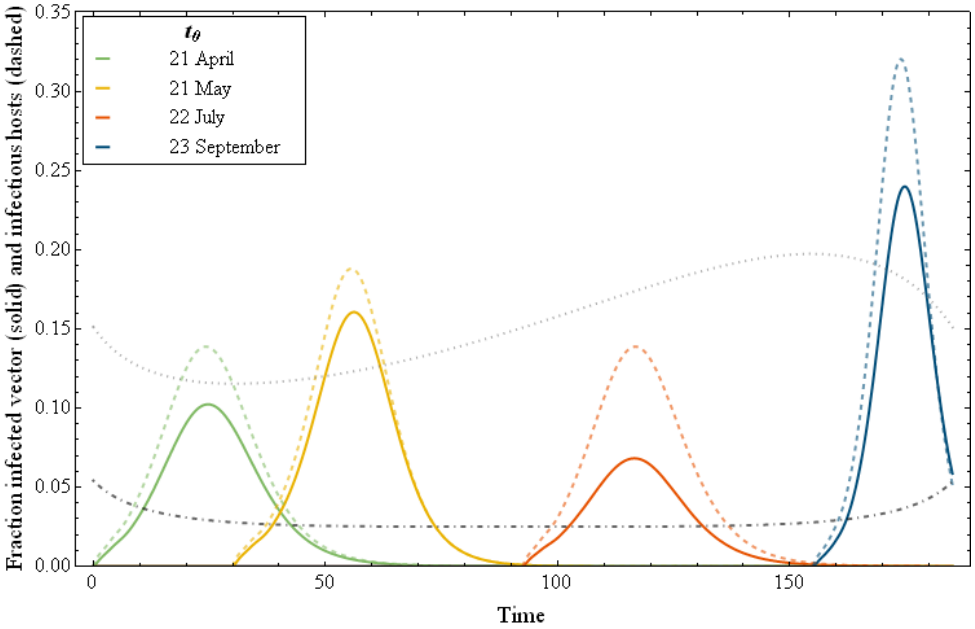

Figure 18. Epidemics for RVFV introduction (t_0) on 21 April, 21 May, 22 July and 23 September with a yearly mean stable-fly to host ratio of 30. Dotted gray line is the relative population size of the stable fly (0.2 is chosen as maximal for graphical reasons). The dashed-dotted line is the mortality rate of the stable fly.

4.4.2. *Anopheles maculipennis*

The risk caused by *An. maculipennis* is found to be low. Only in a few small areas this vector is able to support persistence of RVF (see Figure 19).

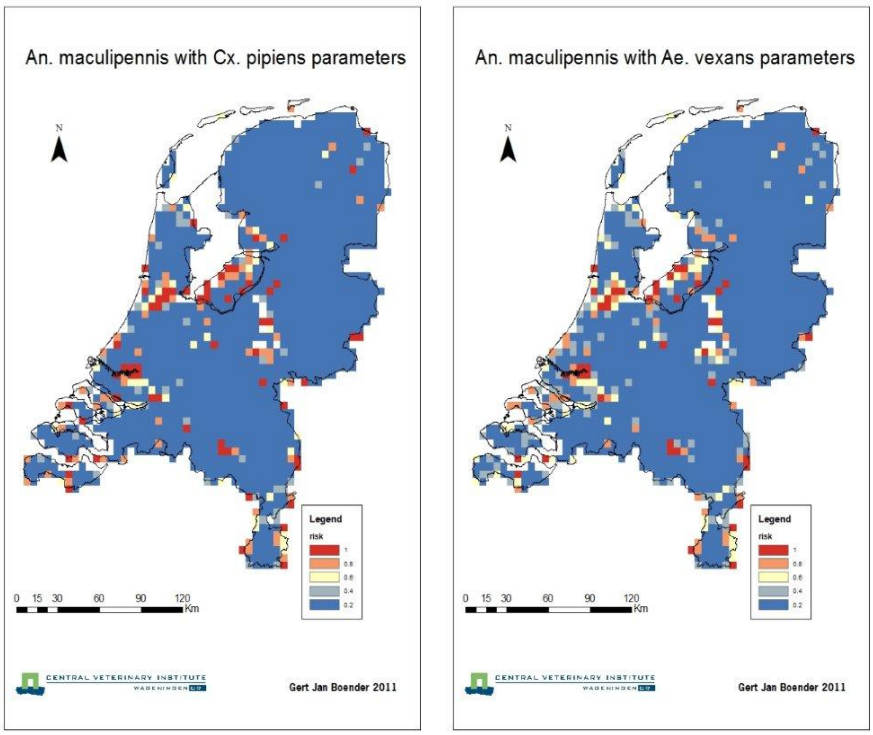

Figure 19. Risk of persistence of RVFV in the Netherlands when *An. maculipennis* complex is the only vector with vector parameters equal to *Cx. pipiens* (left) or *Ae. vexans* (right). Blue indicates a low probability (<20%) of the long term epidemic growth rate exceeding the threshold of 0, and red indicates a high probability (>80%).

4.5. Nature reserve 'De Oostvaardersplassen'

The infection can persist in 'De Oostvaardersplassen' among wildlife (including free range cattle), if deer is a competent host for RVFV or when vectors do not bite deer (Table 6). The first scenario, in which deer is a competent host, will be explored further by deterministic simulation.

Table 6. Host and vector populations in the nature reserve 'De Oostvaardersplassen' and the long term epidemic growth rate for three scenarios: (1) deer is a competent host for RVFV, (2) deer is not a competent host and vectors have an equal preference for cattle and deer, and (3) deer is not bitten by the vector species.

Hosts/km^2 *					Long term epidemic growth rate		
Cattle	Deer	*Ae. vexans*	*Ae. cinereus*	*Cx. pipiens* s.l.	Deer competent	Deer not competent	No deer bitten
10.15	54.30	58.48	99.53	2138.72	0.05	-0.03	0.23

*406 heck cattle and 2,172 red deer at 1st January 2010 in an area of 60 km^2 of which 2/3 is accessible for large herbivores [57].

The total fraction of recovered animals can increase to very high values in the first year of introduction of the infection (Figure 20). The next year we start with the same amount of susceptible, infected and recovered hosts and vectors as at the end of the last season, because we assume that the winter is a period of stasis (i.e. winter survival of the infection). The vertical grey line at time = 185 in Figure 19 marks the end of the first season (23 October) and the beginning of the next season (21 April).

The epidemics can increase to very high values in the following year. With the same assumption of stasis during the winter, it is also shown that introduction late into the season (September) will result in a major epidemic during the next year (blue line in Figure 19).

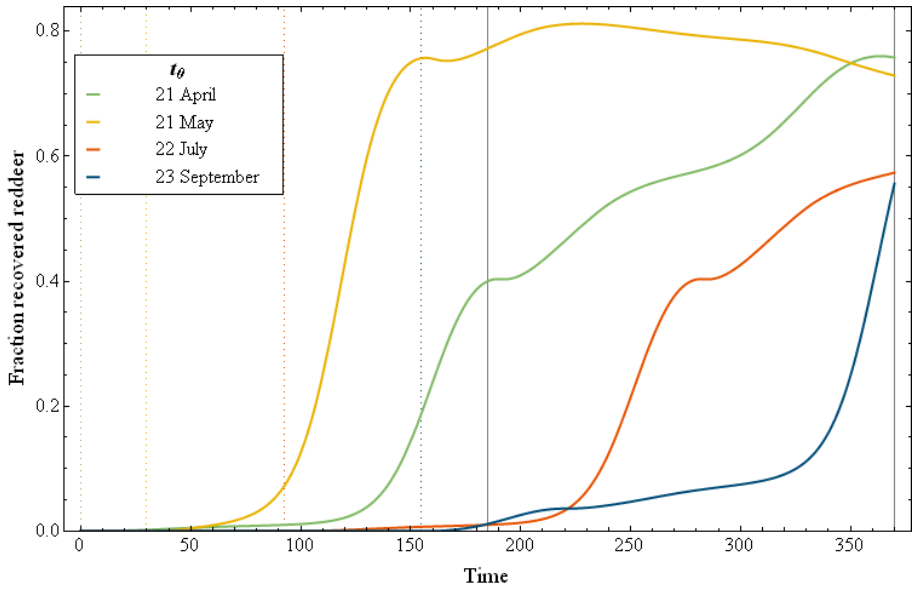

Figure 20. Fraction of red deer recovered from infection for epidemics in the 'Oostvaardersplassen' with RVFV introduction on 21 April (day 0), 21 May, 22 July and 23 September during two vector seasons (marked by gray vertical line). Day of virus introduction is marked by the dotted vertical lines. We assumed that deer is a competent host for RVFV equivalent to cattle, and vector species have an equal preference for cattle and deer.

4.6. Surveillance and collection of data during an epidemic

The risk maps show areas in the Netherlands where a RVF infection can persist (Figure 6) and where outbreaks can occur (Figure 9). These areas are the most important for surveillance purposes.

No differences in host susceptibility and infection parameters between cattle, sheep and goats are described in literature. Only very young animals (less than one week old) have a higher mortality. Increased mortality of very young animals or abortion storms could point out a Rift Valley fever outbreak (see the EMZOO report [55]). However, much debate remains whether RVF is picked up in livestock or due to human cases. Outbreaks in other countries have shown the possibility of a long period in which the disease goes undetected (pers. comm. Prof. Al-Afaleq).

A quantitative assessment of targeted surveillance is currently impossible due to remaining uncertainties regarding spread of RVF in the Netherlands (see the uncertainty analysis of the model, and the unknown transmission between the 5x5 km grid cells), as well as due to missing detailed data on host susceptibility and infection parameters for different host species and age classes. Running experiments in 2011 and beyond (at CVI, Lelystad) may fill in some of these gaps of knowledge on different ages and species in the near future.

For the collection of data during a RVF epidemic, see the report on this subject by van Roermund et al. [58]. In this report, a separate chapter about RVF is described.

5. Discussion

5.1. Risk maps

The study of Rift Valley Fever in the Netherlands shows that areas with a high vector to host ratio are most likely to experience an outbreak and persistence of the infection. Counter-intuitively, these areas are predominantly the sparsely populated livestock areas (SPLAs) in which the observed mosquito numbers were high, probably due to the availability of enough breeding sites (see Figure 6). The vectors (females) in such an area all need blood meals and search for hosts in that area, thus leading to a high vector-host ratio. Outbreaks in these SPLAs with a high vector-host ratio can lead to a high peak in fraction of infectious animals. Depending on the time of the year in which RVFV is introduced, this can peak at 10% (in April, May, September) or even 30% (July) of hosts being infectious.

Outbreaks with a low vector-host ratio are in the densely populated livestock areas (DPLAs). Here, the outbreaks are smaller and the fraction of infectious animals is much lower. However, because these areas contain high livestock numbers, still a considerable number of animals can be affected. These results depend on an important assumption in the model that no other sources than cattle, sheep and goats are present in the area for a blood meal of the mosquitoes. So the mosquitos are forced to look for livestock, and thus livestock numbers play an important role in the vector-host ratio in the model.

The presence of alternative hosts can alter the epidemiology depending on their RVFV competence. A non-competent new host species will reduce the epidemic growth rate strongly (by the 'dilution' effect of the vectors over more host species), while a competent new host species will only reduce the epidemic growth rate mildly, because it only decreases the vector-host ratio.

In the model, mosquito abundances depend on landscape and vegetation (for breeding sites) and are assumed not to be affected by host numbers in the 5 by 5 km areas. However, the presence of many hosts might have an effect on vector densities, e.g. by attraction of vectors from other areas with few hosts, and this can alter the epidemiology [59]. It is unclear whether other host species (such as deer or rodents) are competent hosts for RVFV. When such hosts are competent, a separate cryptic cycle of RVFV can occur in deer (see Figure 19) or rodents.

5.2. The mathematical model & uncertainty analysis

A mathematical model of the spread of Rift Valley Fever after an accidental introduction of the virus was developed for the Netherlands. Transmission was modelled from host to vector and vice versa. An important assumption in the model is that all these hosts and vectors mix homogeneously within the 5 by 5 km areas. In reality, livestock is kept in separate farms and mosquitoes will be unevenly distributed due to habitat preferences within these areas. However, for vector-borne diseases the 'physical' separation of animals in separate farms is by far less strict than for directly transmitted infections (such as FMD or CSF), because mosquitoes fly to and from breeding sites and thus not necessarily back to the same farm or pasture for a blood meal. Random mixing in these small areas is therefore considered not to be too much of an aberration. The size of the areas is based on the minimum resolution in which the vector abundances could be estimated by Avia-GIS [24]. Conveniently, the 5 by 5 km areas correspond to an intervention area around infected farms of approximately 3 km in radius.

Our model was developed to calculate the long term epidemic growth rate, which is an indicator for persistence of the infection. Furthermore, the model was developed to calculate the initial epidemic growth rate at a certain time in the year, which is an indicator for an outbreak to occur or not. The course of the outbreak during time was studied by deterministic simulation. However, persistence, initial epidemic growth rate and the course of an outbreak can only be determined for each 5 by 5 km area. To predict spatial spread *between* areas is not possible with this model.

An advantage of our modelling approach is that with the same set of equations (Ordinary Differential Equations, ODEs, see Eq. 1-16) we can address several aspects of an epidemic: persistence, initial spread, and the course of an outbreak in time. The biological interpretation of the epidemic growth rate (r in day^{-1}) may be less intuitive than the reproduction number R_0, but enables a more straightforward translation from the ODEs. The ODEs can be adapted to include other ways of virus transmission as well, such as direct host-host transmission if it exists in livestock. This is found for RVFV in rodent experiments (Moormann and Kortekaas, pers. comm.).

The advantage of a mathematical model is the study and structured aggregation of current knowledge. With the help of the model, we can both rank parameters in their uncertainty and quantitative show the amount of uncertainty (Figure 4). By taking into account the uncertainty of parameter values in our analysis, it is possible to quantify the likelihood of an area to be at risk of Rift Valley Fever persistence and of an outbreak (see risk maps in Figure 6 and 9).

Our conclusions about persistence of a RVF infection is based on the assumption of stasis during winter. The behaviour of mosquitoes during winter months and how that affects the virus survival is still poorly understood. We assumed that the number of susceptible, infected and recovered hosts and the number of susceptible and infected vectors at the beginning of the vector season is equal to the situation at the end of the previous vector season. This implies that the infection does not die out during the winter. This assumption is valid when mosquitos and/or stable flies are still somewhat active (at least part of the day) during the winter months inside stables, so close to cattle, thus keeping the epidemic going at a very low rate.

Analysis of the model output shows that the results are strongly correlated with the estimated abundance of the vector populations. Three mosquito vectors were taken into account in this study: *Aedes vexans, Aedes cinereus*, and *Culex pipiens* s.l. According to the model, *Cx. pipiens* s.l. contributes by far most to the spread and persistence of RVFV in the Netherlands, (Figure 7), because it is by far the most common mosquito in the country. For the current study we used mosquito trap catches from Belgium, which were extrapolated to the Netherlands using landscape, vegetation, temperature, precipitation and soil data similarities [24]. Thus, trap catches as observed in the Netherlands itself were not used and this gap in knowledge must be filled. Observed trap catch data of the Netherlands by Takken et al (2007) were not sufficient to cover the whole country, and were used in this study to relate mosquito abundances to the average daily (24 h) temperature. Evidently, the vector abundance estimates used in the model need to be more precise to improve the model quantifications.

The parameters determining the vector capacity of *Culex pipiens* s.l. are most important for determining persistence of the infection and of an outbreak. *Culex pipiens* s.l. is modelled here as purely biting on mammals (livestock), and not on birds. The vector capacity for RVFV among livestock would decrease if *Cx. pipiens* s.l. takes blood meals from birds as well, which are not hosts for RVFV. Part of or almost the whole population of *Cx. pipiens* s.l. might be ornithophilic (pers. com. E.J.

Scholte) and the exact species composition of the *Cx. pipiens* s.l. complex in the Netherlands is still unknown. Further studies on host preference and vector competence for RVFV of *Cx. pipiens* s.l. in the Netherlands is most important to decrease the amount of uncertainty in the model. Other endemic mosquito species (e.g. *Anopheles maculipennis*) might be competent vectors for RVFV as well. A better inventory of endemic mosquito species should be made, enabling a better assessment of which mosquitoes might pose a risk. These mosquitoes should be tested for vector competence.

The majority of life history parameters for the vector species (see Tables 2 - 4) was taken from literature, based on observed populations in different countries or continents. Although belonging to the same species, populations in different regions might differ in their life history parameters as well as their vector competence [46]. Temperature dependent parameters such as the longevity of the adult vector can be different between tropical and temperate populations, like in the Netherlands. Furthermore, transmission probabilities from vector to host and vice versa in the model are completely based on hamster experiments (and not on cattle or sheep), which is known to be very susceptible to Rift Valley Fever. In some cases, the host preference of the vector was based on blood meal analysis without knowing the underlying host population sizes. This biases the estimate towards the more abundant host species in the studied areas. Unfortunately, this is the only data available when choice experiments of the vector were not done.

Vertical transmission of the virus from adult *Aedes vexans* vectors to eggs has almost no effect on an outbreak and even not on persistence of the infection, because of the minor role of this vector species in the transmission in the Netherlands (Figure 7). Furthermore, the phenomenon of vertical transmission is subject to controversy. To our knowledge only one report [44] suggests the possibility of transmission via eggs in a related vector species, *Ae. linneatopennis*, which is not present in Europe. Studies that reproduce these findings under laboratory conditions are unknown to our knowledge [4].

The collection of literature data on mosquito life history parameters was time consuming. Several other future studies and risk estimates will need this information as well. A separate study collecting these parameter estimates for all mosquito species in the Netherlands is recommended to avoid ad hoc studies and duplication of work.

5.3. Effect of control measures

5.3.1. Culling

The current policy (Concept-Beleidsdraaiboek Rift Valley fever, version 1.0, 2009) is culling of all ruminants on infected farms. During past outbreaks (FMD and CSF), preventive culling of animals in the neighbourhood was done to prevent infections to spread to other farms, but this policy has been changed to ring-vaccination for FMD and CSF, and is not mandatory for RVF.

Although culling can be efficient for directly transmitted diseases (like CSF or FMD), for vector-borne diseases culling of hosts will increase the vector-host ratio in that area, and that increases the epidemic growth rate in the remaining animal population. Another possibility is that infected vectors will increase the area in which they search for hosts, and thereby increasing the transmission to other farms. Hence, preventive culling will only be an option if *all* hosts within the flight range of infected vectors are removed.

In case of an on-going outbreak, culling also removes part of the infected animals. In that situation, not only the vector-host ratio is increased, but also the average length of the infectious period is reduced due to the culling of infectious animals. This effect will counter-act and reduce the epidemic growth rate. Indeed, our simulations show that culling of hosts shortens an outbreak (if in a less favourable season like May), depending on the culling strategy and on the detection delay (see Figure 11). This effect is important, because a shorter outbreak affecting a smaller number of hosts decreases the probability that the infection spreads to other areas.

However, culling also increases the fraction of infectious vectors, and this might have an important effect on the spread to other areas. Livestock movement can be regulated, but vector movement cannot. Additionally, by culling and thus removing livestock from an area, vectors might be more prone to disperse to other areas. Culling of livestock might increase the infection pressure for other areas or for other animal species (including humans).

A more detailed investigation of the effects of culling during outbreaks of vector-borne diseases is done in another modelling study [2]. Different culling strategies were investigated for a generic vector-borne infection. The main conclusion of that study is that culling is a dangerous strategy for vector-borne diseases, because the balance between positive and negative effects is hard to asses prior to an outbreak. Only when culling of viraemic (i.e. infectious) animals is feasible, culling of these animals can reduce the impact and duration of an outbreak. For RVF, this seems to be unfeasible in practice due to the high biosafety procedures which should be in place to work with blood of infectious animals (pers. comm. R. Moormann).

5.3.2. Vaccination

The critical vaccination degree for the host population to prevent an RVF outbreak or persistence depends on the vector-host ratio in the area, and thus on the time during the year that the outbreak occurs. The critical vaccination degree increases steeply with vector-host ratio to above 90% of the animals. This critical vaccination degree was determined assuming a perfect vaccine, which protects animals from becoming infectious. Imperfect vaccines that only protect animals from clinical signs (disease) do not necessarily result in a decrease in susceptibility of the uninfected animal and/or infectivity of the infected animal [60]. The focus of vaccine development should be on both preventing clinical protection and prevention of transmission.

5.3.3. Vector control

Vector control aiming at a complete prevention of a RVF outbreak or of persistence requires a strong reduction of the vector population (>90%). The required reduction in vector abundance is more easily reached in a DPLA than in an SPLA. However, also in an SPLA a reduction in vector abundance decreases the (long term) epidemic growth rate, thus enhancing the effect of other control strategies. Vector control could for instance bring the vector-host ratio in a lower range for which the critical vaccination degree is more easily reached (vaccination degree being the % of animals protected from infection after vaccination).

Vector control can be applied by the use of environmental-friendly larvicides. Experience with exotic mosquitoes has shown that they can be (almost) eradicated [61], showing that local eradication of a mosquito species is possible. However, the delay between the use of larvicides and reduction of the adult vector population to 95% can be calculated to be 50 to 100 days, based on the life span of 18 to 32 days for

adult mosquitoes. For an on-going outbreak, adulticides are more interesting for a rapid control.

5.4. *Stomoxys calcitrans* and *Anopheles macullipennis*

The role of the stable fly *Stomoxys calcitrans* in transmitting RVFV during an outbreak is unknown. Our investigations show that the stable fly poses a potential risk for an RVF outbreak, if competent as mechanical vector. Given the assumptions underlying our calculations, very low densities of this vector (of only a few per cow) are able to support a persistent infection by keeping the long term epidemic growth rate above the threshold of 0.

In contrast to mosquitoes, stable flies are less likely to disperse over large areas, as their preferred breeding sites consist of straw, hay and manure [62]. Hence, stable flies do not have to leave a farm to find suitable breeding sites. The end of outbreaks driven by stable flies will therefore be caused by local depletion of susceptible hosts (Figure 18). The stable fly will most likely act as an amplifying vector on a local farm: after introduction of the infection by a mosquito vector, the infection spreads very fast from animal to animal due to the presence of stable flies. Stable flies should be monitored during a RVF epidemic, due to the high fraction of infectious flies.

The mosquito *An. macullipennis* is not likely to contribute to the risk of a RVF epidemic in the Netherlands. However, the presence of any another competent vector should not be dismissed.

5.5. Nature reserve 'De Oostvaardersplassen'

A RVF outbreak and persistence of the infection can occur in a nature reserve like the Oostvaardersplassen, when either deer species are a competent host or deer are not preferred by vectors (Table 6). To our knowledge no deer species have been tested for RVFV competence. Furthermore, the preference of vectors for deer is unknown. Natural mortality is high among wildlife (ca 30% per year in the Oostvaarders-plassen), hence replacement of recovered animals by new susceptible animals is also high. This process enables the infection to persist by an influx of new susceptible animals. Additionally, due to the high natural mortality of hosts, a RVF outbreak in a nature reserve is very likely to remain unobserved, especially in the Oostvaarders-plassen as this is an area with a policy of minimal intervention by man. Therefore, monitoring of wildlife should be commenced during a RVF outbreak.

When deer are competent hosts, introduction of the infection in the beginning of the season (April) can lead to high fractions of infected deer and free range cattle (Figure 19). Red deer and free range cattle are confined to the nature reserve, but the smaller roe deer might migrate and pose a risk for livestock in other areas and humans.

6. Conclusions

Risk maps

- Parts of the Netherlands are at risk of a RVF outbreak and of persistence of the infection according to present knowledge and assuming that *Ae. vexans, Ae. cinereus*, and *Cx. pipiens* s.l. are competent RVFV vectors. Counter-intuitively, these are the sparsely populated livestock areas (SPLA), due to the high vector-host ratios in these areas.

Uncertainty and data-gaps

- It is important to know which species of arthropods are competent vectors for RVFV in the Netherlands. The main focus should be addressed to species associated with livestock and/or wildlife.
- The vector-host ratio is most important in determining the risk of a RVF outbreak and of persistence of the infection in an area.
- The model output is strongly correlated with the estimated vector abundances. Vector trap catches from the Netherlands itself were not used in this study, but observed data from Belgium were extrapolated. This gap in knowledge must be solved by vector monitoring in the Netherlands (by f.i. the Centre for Monitoring of Vectors, Wageningen).
- *Culex pipiens* s.l. contributes by far most to the spread and persistence of RVFV in the Netherlands, according to the model. Further studies on vector competence for RVFV, abundance and host preference of *Cx. pipiens* s.l. in the Netherlands are most important to decrease the amount of uncertainty in the model.

Control

- If vaccination is chosen as intervention strategy, a high vaccination degree (>90% of animals protected from infection) is needed to prevent RVF outbreaks throughout the year.
- Vector control (by larvicides or adulticied) can be a helpful tool to reduce the epidemic growth rate of RVF. However, very high reductions of vector populations (>90%) are needed when this is the only intervention strategy to prevent an outbreak or to prevent persistence.
- Culling of animals is a dangerous intervention strategy, because of the possibility of unpredictable negative effects, like a larger outbreak or an increase of the infection pressure to other areas / farm.

Nature reserves

- The wildlife populations (including free range cattle) in the nature reserve 'Oostvaardersplassen' can sustain a RVF infection, when either deer species are a competent host or deer are not preferred by vectors. The host competence of deer species for RVF should be determined.
- Wildlife, such as deer and rodents (especially rats), can be a reservoir of RVF and surveillance during an outbreak is warranted.

Surveillance

- Monitoring of all biting arthropods, such as mosquitoes, midges, stable flies and ticks, present in the stable or meadow of infected farms should be done during a RVF outbreak.
- Samples of potential mechanical vectors (such as stable flies and ticks) should be processed rapidly in the lab, as virus is quickly denaturated.

Acknowledgements

This research was funded by the Ministry of Agriculture, Nature and Food Quality (LNV, now EL&I) in the Netherlands (project BO-08-010-022). The authors would like to thank W. van Bortel and V. Versteirt (ITG Antwerp) for mosquito observation data from Belgium, E.J. Scholte and J. Beeuwkes of the Center Monitoring Vectors for discussions about mosquito abundances and behaviour. R. Moormann, J. Kortekaas (CVI, Lelystad) and J.W. Zijlker (EL&I) for discussions about Rift Valley fever.

References

1. Hoek, M.R., G.J. Boender, and C.J. de Vos, *Risk of introducing Rift Valley fever virus into the Netherlands A qualitative risk assessment*. 2011, Lelystad: CVI- Wageningen UR Report number: 11/CVI0039.
2. Fischer, E.A.J., *When culling of livestock makes vector-borne diseases less controllable.* In prep.
3. Pepin, M., et al., *Rift Valley fever virus(Bunyaviridae: Phlebovirus): an update on pathogenesis, molecular epidemiology, vectors, diagnostics and prevention.* Vet Res, 2010. **41**(6): p. 61.
4. Swanepoel, R. and J.A.W. Coetzer, *Rift Valley Fever*, in *Infectious Diseases of Livestock*, J.A.W. Coetzer and R.C. Tustin, Editors. 2004, Oxford University Press Southern Africa: Cape Town.
5. Chevalier, V., et al., *Rift Valley fever--a threat for Europe?* Euro Surveill, 2010. **15**(10): p. 19506.
6. Balkhy, H.H. and Z.A. Memish, *Rift Valley fever: an uninvited zoonosis in the Arabian peninsula.* Int J Antimicrob Agents, 2003. **21**(2): p. 153-7.
7. Al-Hazmi, A., et al., *Ocular complications of Rift Valley fever outbreak in Saudi Arabia.* Ophthalmology, 2005. **112**(2): p. 313-8.
8. Daubney, R., J.R. Hudson, and P.C. Garnham, *Enzootic hepatitis or rift valley fever. An undescribed virus disease of sheep cattle and man from east africa.* The Journal of Pathology and Bacteriology, 1931. **34** (4): p. pages 545–579.
9. Gargan, T.P., et al., *Vector Potential of Selected North-American Mosquito Species for Rift-Valley Fever Virus.* American Journal of Tropical Medicine and Hygiene, 1988. **38**(2): p. 440-446.
10. Moutailler, S., et al., *Potential vectors of Rift Valley fever virus in the Mediterranean region.* Vector Borne Zoonotic Dis. , 2008. **8**: p. 749–754.
11. Turell, M.J., et al., *Vector competence of selected African mosquito (Diptera: Culicidae) species for Rift Valley fever virus.* J Med Entomol, 2008. **45**(1): p. 102-8.
12. Madder, D.J., G.A. Surgeoner, and B.V. Helson, *Number of Generations, Egg-Production, and Developmental Time of Culex-Pipiens and Culex-Restuans (Diptera, Culicidae) in Southern Ontario.* Journal of Medical Entomology, 1983. **20**(3): p. 275-287.
13. Keeling, M.J. and P. Rohani, *Modeling infectious diseases in humans and animals*2008.
14. KNMI. *Royal Netherlands Meteorological Institute (KNMI)*. 2010 2011 [cited 2010 September 1]; Available from: http://www.knmi.nl/climatology/daily_data/download.html.
15. Coetzer, J.A.W. and R.C. Tustin, *Infectious Diseases of Livestock*. Vol. 2. 2004, Cape Town: Oxford University Press Southern Africa.
16. Davies, F.G. and L. Karstad, *Experimental infection of the African buffalo with the virus of Rift Valley fever.* Trop Anim Health Prod, 1981. **13**(4): p. 185-8.
17. Evans, A., et al., *Prevalence of antibodies against Rift Valley fever virus in Kenyan wildlife.* Epidemiol Infect, 2008. **136**(9): p. 1261-9.

18. Easterday, B.C., L.C. Murphy, and D.G. Bennett, *Experimental Rift Valley Fever in Calves, Goats, and Pigs.* American Journal of Veterinary Research, 1962. **23**(97): p. 1224-&.
19. Anonymous, *Opinion of the Scientific Panel on Animal Health Welfare on a request from the Commission related to "The Risk of a Rift Valley Fever Incursion and its Persistence in the Community"*. 2005: EFSA Report number: EFSA-Q-2004-050.

20. Fischer, E.A.J., et al., *Appendix 4 Scenario studies for vector-borne zoonoses*. 2010, Bilthoven: RIVM, CVI-Wageningen UR, Universiteit Utrecht, GD Report number.

21. McIntosh, B.M., D.B. Dickinson, and I. dos Santos, *Rift Valley fever. 3. Viraemia in cattle and sheep. 4. The susceptibility of mice and hamsters in relation to transmission of virus by mosquitoes.* J S Afr Vet Assoc, 1973. **44**(2): p. 167-9.
22. Olaleye, O.D., O. Tomori, and H. Schmitz, *Rift Valley fever in Nigeria infections in domestic animals.* Revue Scientifique Et Technique De L Office International Des Epizooties, 1996. **15**(3): p. 937-946.
23. Swanepoel, R., et al., *Comparative Pathogenicity and Antigenic Cross-Reactivity of Rift-Valley Fever and Other African Phleboviruses in Sheep.* Journal of Hygiene, 1986. **97**(2): p. 331-346.
24. Ducheyne, E. and G. Hendrickx, *Abundance modeling of mosquito and biting midge species in the Netherlands*. 2010, Zoersel, Belgium: AVIA GIS Report number: 28.

25. Jupp, P.G., et al., *The 2000 epidemic of Rift Valley fever in Saudi Arabia: mosquito vector studies.* Medical and Veterinary Entomology, 2002. **16**(3): p. 245-252.
26. Hoch, A.L., T.P. Gargan, 2nd, and C.L. Bailey, *Mechanical transmission of Rift Valley fever virus by hematophagous Diptera.* Am J Trop Med Hyg, 1985. **34**(1): p. 188-93.
27. Bailey, C.L., et al., *Winter Survival of Blood-Fed and Nonblood-Fed Culex-Pipiens L.* American Journal of Tropical Medicine and Hygiene, 1982. **31**(5): p. 1054-1061.
28. Carron, A., et al., *Survivorship characteristics of the mosquito Aedes caspius adults from southern France under laboratory conditions.* Med Vet Entomol, 2008. **22**(1): p. 70-3.
29. Costello, R.A. and R.A. Brust, *Longevity of Aedes-Vexans Diptera-Culicidae under Different Temperatures and Relative Humidities in Laboratory.* Journal of Economic Entomology, 1971. **64**(1): p. 324-&.
30. Wonham, M.J., T. de-Camino-Beck, and M.A. Lewis, *An epidemiological model for West Nile virus: invasion analysis and control applications.* Proceedings of the Royal Society of London Series B-Biological Sciences, 2004. **271**(1538): p. 501-507.
31. Gad, A.M., et al., *Survival Estimates for Adult Culex-Pipiens in the Nile Delta.* Acta Tropica, 1989. **46**(3): p. 173-179.
32. Faran, M.E., et al., *Reduced Survival of Adult Culex-Pipiens Infected with Rift-Valley Fever Virus.* American Journal of Tropical Medicine and Hygiene, 1987. **37**(2): p. 403-409.

33. Lysyk, T.J., *Relationships between temperature and life-history parameters of Stomoxys calcitrans (Diptera : Muscidae).* Journal of Medical Entomology, 1998. **35**(2): p. 107-119.
34. Ba, Y., et al., *Feeding pattern of Rift Valley Fever virus vectors in Senegal. Implications in the disease epidemiology [Comportement trophique des vecteurs du virus de la fièvre de la Vallée du Rift au Sénégal: Implications dans l'épidémiologie de la maladie]*. Bulletin de la Societe de Pathologie Exotique 2006. **99**(4): p. 283-289.
35. Briegel, H., A. Waltert, and A.R. Kuhn, *Reproductive physiology of Aedes (Aedimorphus) vexans (Diptera: Culicidae) in relation to flight potential.* J Med Entomol, 2001. **38**(4): p. 557-65.
36. Ndiaye, P.I., et al., *Rainfall triggered dynamics of Aedes mosquito aggressiveness.* Journal of Theoretical Biology, 2006. **243**(2): p. 222-229.
37. Meegan, J.M., et al., *Experimental transmission and field isolation studies implicating Culex pipiens as a vector of Rift Valley fever virus in Egypt.* Am J Trop Med Hyg, 1980. **29**(6): p. 1405-10.
38. Turell, M.J., T.P. Gargan, and C.L. Bailey, *Replication and Dissemination of Rift-Valley Fever Virus in Culex-Pipiens.* American Journal of Tropical Medicine and Hygiene, 1984. **33**(1): p. 176-181.
39. Turell, M.J., T.P. Gargan, and C.L. Bailey, *Culex-Pipiens (Diptera, Culicidae) Morbidity and Mortality Associated with Rift-Valley Fever Virus-Infection.* Journal of Medical Entomology, 1985. **22**(3): p. 332-337.
40. Patrican, L.A. and C.L. Bailey, *Ingestion of immune bloodmeals and infection of Aedes fowleri, Aedes mcintoshi, and Culex pipiens with Rift Valley fever virus.* Am J Trop Med Hyg, 1989. **40**(5): p. 534-40.
41. Turell, M.J., et al., *Vector competence of Egyptian mosquitoes for Rift Valley fever virus.* American Journal of Tropical Medicine and Hygiene, 1996. **54**(2): p. 136-139.
42. Turell, M.J., *Effect of Environmental-Temperature on the Vector Competence of Aedes-Taeniorhynchus for Rift-Valley Fever and Venezuelan Equine Encephalitis Viruses.* American Journal of Tropical Medicine and Hygiene, 1993. **49**(6): p. 672-676.
43. Gad, A.M., et al., *Rift-Valley Fever Virus Transmission by Different Egyptian Mosquito Species.* Transactions of the Royal Society of Tropical Medicine and Hygiene, 1987. **81**(4): p. 694-698.
44. Linthicum, K.J., et al., *Rift-Valley Fever Virus (Family Bunyaviridae, Genus Phlebovirus) - Isolations from Diptera Collected during an Inter-Epizootic Period in Kenya.* Journal of Hygiene, 1985. **95**(1): p. 197-209.
45. Hamer, G.L., et al., *Host Selection by Culex pipiens Mosquitoes and West Nile Virus Amplification.* American Journal of Tropical Medicine and Hygiene, 2009. **80**(2): p. 268-278.
46. Medlock, J.M., K.R. Snow, and S. Leach, *Potential transmission of West Nile virus in the British Isles: an ecological review of candidate mosquito bridge vectors.* Medical and Veterinary Entomology, 2005. **19**(1): p. 2-21.
47. Gad, A.M., et al., *Host feeding of mosquitoes (Diptera : Culicidae) associated with the recurrence of Rift Valley fever in Egypt.* Journal of Medical Entomology, 1999. **36**(6): p. 709-714.
48. Platonov, A.E., et al., *Epidemiology of West Nile infection in Volgograd, Russia, in relation to climate change and mosquito (Diptera: Culicidae) bionomics.* Parasitology Research, 2008. **103**: p. S45-S53.

49. Hartemink, N., et al., *Mapping the basic reproduction number (R0) for vector-borne diseases: a case study of bluetongue virus.* Epidemics, 2009. **1**(3).
50. Campbell, J.B., et al., *Effects of stable flies (Diptera : Muscidae) on weight gains of grazing yearling cattle.* Journal of Economic Entomology, 2001. **94**(3): p. 780-783.
51. Lysyk, T.J., *Temperature and population density effects on feeding activity of Stomoxys calcitrans (Diptera: Muscidae) on cattle.* J Med Entomol, 1995. **32**(4): p. 508-14.
52. Mullens, B.A., et al., *Behavioural responses of dairy cattle to the stable fly, Stomoxys calcitrans, in an open field environment.* Medical and Veterinary Entomology, 2006. **20**(1): p. 122-137.
53. Takken, W., et al., *Distribution and dynamics of arthropod vectors of zoonotic disease in The Netherlands in relation to risk of disease transmission. Report of project TRC2005/2867 of the Ministry of Agriculture, Nature Conservation and Food Security.* 2007, Wageningen: Laboratory of entomology, Wageningen UR Report number: TRC2005/2867 55 pp.
54. Naslund, J., et al., *Kinetics of Rift Valley Fever Virus in experimentally infected mice using quantitative real-time RT-PCR.* Journal of Virological Methods, 2008. **151**(2): p. 277-282.
55. Braks, M., et al., *Scenario studies for vector-borne zoonoses*, in *Emerging zoonoses: early warning and surveillance in the Netherlands. RIVM-rapport 330214002*, J. Van der Giessen, A. van de Giessen, and M. Braks, Editors. 2010.
56. Miller, W.S. and M.S. Artenstein, *Aerosol stability of three acute respiratory disease viruses.* Proc Soc Exp Biol Med, 1967. **125**(1): p. 222-7.
57. www.staatsbosbeheer.nl. [cited 2010 28-12-2010]; Available from: http://www.staatsbosbeheer.nl/Nieuws%20en%20achtergronden/Dossiers/Oostvaardersplassen/Feiten%20en%20cijfers.aspx.
58. Van Roermund, H.J.W., et al., *Gegevensverzameling tijdens een epidemie*. 2011 Lelystad: Central Veterinary Institute, part of Wageningen UR Report number: 11/CVI0041 78 pp (incl 5 appendices).
59. Lord, C.C., C.R. Rutledge, and W.J. Tabachnick, *Relationships between host viremia and vector susceptibility for arboviruses.* Journal of Medical Entomology, 2006. **43**(3): p. 623-630.
60. Lord, C.C., et al., *Vector-borne diseases and the basic reproduction number: A case study of African horse sickness.* Medical and Veterinary Entomology, 1996. **10**(1): p. 19-28.
61. Scholte, E., et al., *Introduction and control of three invasive mosquito species in the Netherlands, July-October 2010.* Euro Surveill, 2010. **15**(45).
62. Bishopp, F.C., *The stable fly (Stomoxys calcitrans L.), an important live stock pest.* Journal of Economic Entomology, 1913. **6**: p. 112-128.
63. Heesterbeek, J.A.P. and M.G. Roberts, *Threshold Quantities for Infectious Diseases in Periodic Environments.* Journal of Biological Systems, 1995. **3**(3): p. 779-787.
64. Klausmeier, C.A., *Floquet theory: a useful tool for understanding nonequilibrium dynamics.* Theoretical Ecology, 2008. **1**(3): p. 153-161.
65. Floquet, M.G., *Sur les équations différentielles linéaires à coefficients périodiques.* Ann Ecole Norm Sup, 1883. **12**: p. 47-88.

66. Shirley, J.H., *Solution of Schrodinger Equation with a Hamiltonian Periodic in Time.* Physical Review, 1965. **138**(4B): p. B979-&.
67. Boender, G.J., S. Vega, and H.J.M. De Groot, *A physical interpretation of the Floquet description of magic angle spinning nuclear magnetic resonance spectroscopy.* Molecular Physics, 1998. **95**(5): p. 921-934.
68. Oppenheim, A.V., A.S. Willsky, and I.T. Young, *Signals and Systems*1983: Prentice Hall.
69. Alonso, M. and E.J. Finn, *Quantum and Statistical Physics*. Fundamental University Physics. Vol. III. 1968: Addison Wesley.

Appendix: Floquet formalism

Introduction

The transmission of an infection between hosts via a vector is periodic in time due to specific properties of the vector population. Properties such as vector abundance and activity are seasonal, due to their dependence on temperature, day length and/or state of the soil and vegetation. Thus, seasonal variation is inherently coupled with vector-borne infections

To deal with such annually recurring patterns, we propose to use the Floquet theory, which helps in analysing the long term, *multiannual* (in)stability of a dynamic system. The Floquet theory is the study of systems of linear differential equations with periodic coefficients, and can be used to determine the stability of equilibria. Application to the field of epidemiology has been proposed previously [63]. However, the use of the Floquet theory in ecology and epidemiology is still limited today, and if used, they always make use of numerical solutions of the linearized system of periodic ODE's [64]. This is a straightforward and easily implemented method, but it is not proven to be valid for more complex systems (involving multiple time dependent parameters).

We have applied the Floquet theory to a vector-borne infection system with seasonally varying parameters. We show that the *long term* epidemic growth rate of an infection can be disentangled from periodic fluctuations in epidemic growth rate. To do so, we apply the Floquet theory (Part A), and incorporate properties of the Fourier series (Part B). Finally, a numerical example is given using the derived algorithm (Part C). This extensive and rather complicated appendix is required to discuss the method and to prove its validity.

Fortunately, after a lot of technical work, we can end up with a final algorithm (presented in Part C), which is relatively simple and can easily be used in computer calculations to determine stability and long term growth of a specific system.

Part A: Physical framework for periodic fluctuations in transmission of a vector-borne infection

We apply the Floquet theory to determine the stability of the infection-free equilibrium of a vector-borne infection, i.e. to see if an introduced virus can persist for a longer time period. To do so, the method evaluates the long term behaviour of the system, by separating this from the short term (periodic) behaviour of the system . The method is straight forward, in the sense that the long term behaviour of a system is described directly by the Floquet exponents. If the largest of the Floquet exponents is larger than 0, the infection-free equilibrium is unstable, and infections can successfully invade in such a system. Thus we conclude that the infection can persist for an extended time period. The Floquet exponents are the real parts of the (possibly complex) eigenvalues of the Floquet transmission operator $\mathbf{K_F}$ which we define later in this appendix (EquationA.7).

To visualize the concept of the separation of the long and short time behaviour, we visualised an example in Figure 1, where the dashed-line describes the long term behaviour of a very simple model for epidemic growth with a recurring (seasonal) variability (sin t) in one of the parameters (a): ($v(t) = v_0 \exp(r\, t + \mathrm{a} \sin(2\, \pi\, t))$.

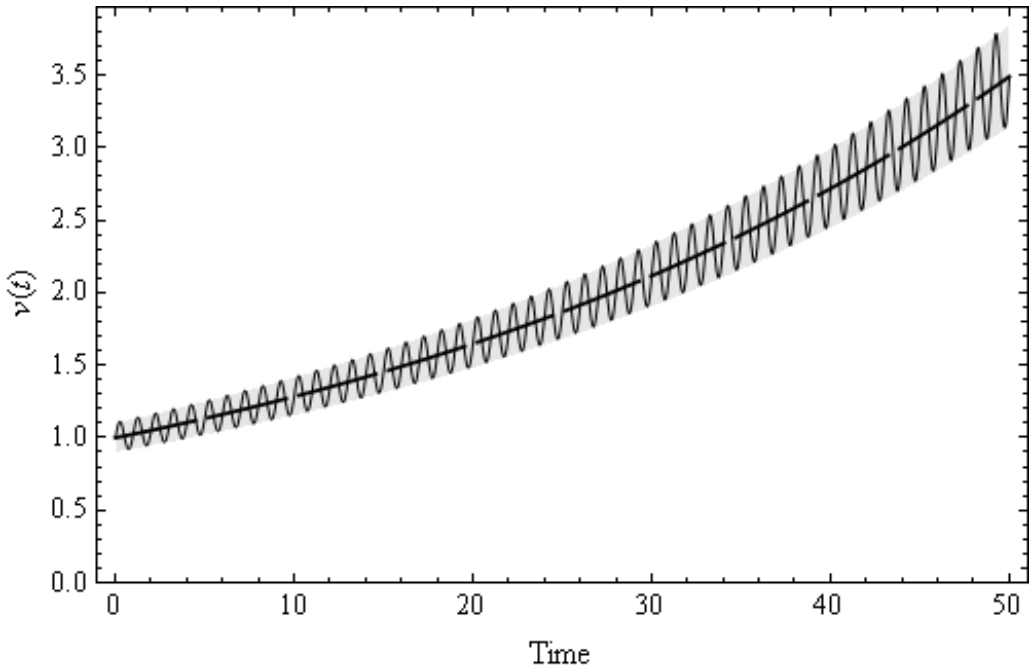

Figure 21. Example of a simple model with a periodic epidemic growth. The dashed line illustrates the long term epidemic growth, which is represented by the positive Floquet exponent. The solid line is the actual epidemic size, fluctuating due to seasonality. Time is in years.

For epidemiological purposes, we are interested in the stability of the infection-free equilibrium, i.e. a population without infecteds. Infecteds are all hosts and vectors that are infected with the infectious agent, hence the infection-free equilibrium means no infected hosts or vectors. The infection-free equilibrium is stable, when the long term growth rate of the population of infecteds is smaller than 0.

Due to seasonal aspects, the changes in the population of infecteds is time dependent. The time dependency of the change in the population of infecteds is

$$\frac{\partial}{\partial t} v(\varphi_0, t) = \mathrm{K}(\varphi_0, t) v(\varphi_0, t), \qquad \text{(A.1)}$$

in which $v(\varphi_0, t)$ is the state describing the population of infecteds, **K** the periodic transmission operator and t the epidemic time (i.e. time since start of epidemic), φ_0 the initial phase, which depends on the moment in the season at which the epidemic starts.

The mathematical solution of Equation (A.1) is presented by Floquet [65]. This solution is applied in physics to solve the Schrödinger equation for a period Hamiltonian operator, which describes the energy of a system. This solution leads to the Floquet Theory [66, 67]. We apply this to the field of epidemiology. To disentangle periodic changes and the long term epidemic growth rate, we will need some algebra to prove that our numerical algorithm in Part C is valid.

At the start of an epidemic one infected is present in a further completely susceptible population, and this initial state will be denoted by v_0. The introduction of the infection can be at any time in the season. Therefore, this state v_0 is independent of t and φ_0.

The transmission operator, $\mathbf{K}(\varphi_0, t)$, is periodic, and can be expanded in a Fourier series [68]:

$$\mathrm{K}(\varphi_0, t) = \sum_{p=-\infty}^{\infty} \mathrm{K}_p \exp(ip\varphi_0 + ip\omega_r t), \tag{A.2}$$

with $\omega_r = 2\pi/T_r$. T_r is the length of the period. In the case of annual periodicity, T_r is the rotation period of the earth around the sun.

To describe this rotation, we need to replace the initial phase φ_0, which is a constant and thus not differentiable. The constant initial phase is replaced by a (differentiable) phase variable φ for the calculation (see Equations B.8 and B.9 in Part B). This phase variable φ can be transformed back to the initial phase φ_0, accordingly.

$$\begin{aligned} v(\varphi_0, t) &= \int_{-\pi}^{\pi} v(\varphi, t)\delta(\varphi - \varphi_0)d\varphi \\ &= \sum_{m=-\infty}^{\infty} \tfrac{1}{\sqrt{2\pi}} \exp(-im\varphi_0) \int_{-\pi}^{\pi} v(\varphi, t)\Phi_m(\varphi)d\varphi \end{aligned} \tag{A.3}$$

in which the Fourier states $\Phi_m(\varphi)$ and the unit impulse function δ are introduced in part B.

According to Equation (A.1), $v(\varphi, t)$ is the solution of the equation

$$\begin{aligned} \frac{\partial}{\partial t} v(\varphi, t) &= \mathbf{K}(\varphi, t)v(\varphi, t) \\ \frac{\partial}{\partial t} \mathbf{U}(\varphi, t)v_0 &= \mathbf{K}(\varphi, t)\mathbf{U}(\varphi, t)v_0 \end{aligned} \tag{A.4}$$

in which the evolution operator $\mathbf{U}(\varphi, t)$ describes the development of the system in time, and is defined by

$$v(\varphi, t) = \mathbf{U}(\varphi, t)v_0 \tag{A.5}$$

In the following section we rewrite the operator part of Equation (A.4), i.e. without constant v_0. This results in disentanglement of the transmission operator $\mathbf{K}(\varphi,0)$ and the rotating period ω_r in Equation (A.6). Substitution of the outcome in Equation (A.4) transforms the whole equation to a rotation frame, in which the transmission operator becomes time independent (A.7). And this equation can be solved (A.8). After substitution of this solution in (A.3), the variable φ is transformed back to constant φ_0 leading to $v(\varphi_0, t)$, the state describing the population of infecteds (A.11).

To rewrite the operator part of Equation (A.4) to a constant transmission operator in a rotating frame, we use the relations derived in Part B. The change in the operator due to a rotation around the sun is described by $\mathbf{L}_z$, which is called the angular momentum operator in quantum mechanics (Equation B.1) and the Fourier operator, $\mathbf{F}_p$, is $\exp(ip\varphi)$ (Equation B.3).

The operator part of (A.4) can be rewritten as

$$
\begin{aligned}
&\frac{\partial}{\partial t}\mathbf{U}(\varphi,t)-\mathbf{K}(\varphi,t)\mathbf{U}(\varphi,t)= \\
&\frac{\partial}{\partial t}\mathbf{U}(\varphi,t)-\left(\sum_{p=-\infty}^{\infty}\mathbf{K}_p\exp(ip\varphi+ip\omega_{\mathrm{r}}t)\right)\mathbf{U}(\varphi,t)= \\
&\frac{\partial}{\partial t}\mathbf{U}(\varphi,t)-\left(\exp(i\omega_{\mathrm{r}}\mathbf{L}_z t)\left(\sum_{p=-\infty}^{\infty}\mathbf{K}_p\mathbf{F}_p\right)\exp(-i\omega_{\mathrm{r}}\mathbf{L}_z t)\right)\mathbf{U}(\varphi,t)= \\
&\frac{\partial}{\partial t}\mathbf{U}(\varphi,t)-\left(\exp(i\omega_{\mathrm{r}}\mathbf{L}_z t)\mathbf{K}(\varphi,0)\exp(-i\omega_{\mathrm{r}}\mathbf{L}_z t)\right)\mathbf{U}(\varphi,t)
\end{aligned}
\tag{A.6}
$$

In this derivation the Fourier expansion of the transmission operator (A.2), the definition of the Fourier operator (B.2) and the relation of the Fourier operator and the Angular Momentum operator, $\mathbf{L}_z$, are applied. Now we see that the transmission operator $\mathbf{K}(\varphi,0)$ is disentangled from the rotation with ω_{r} around the z-axis (the rotation around the sun), which is described by the exponential operator $\exp(i\omega_{\mathrm{r}}\mathbf{L}_z t)$. To transform the total equation to the rotating frame we substituted $\mathbf{U}(\varphi,t)=\exp(i\omega_{\mathrm{r}}\mathbf{L}_z t)\mathbf{U}_F(\varphi,t)$ in which $\mathbf{U}_F(\varphi,t)$ is the Floquet evolution operator in Equation (A.5) . With some algebra,

$$
\begin{aligned}
&\frac{\partial}{\partial t}\exp(i\omega_{\mathrm{r}}\mathbf{L}_z t)\mathbf{U}_F(\varphi,t)-(\exp(i\omega_{\mathrm{r}}\mathbf{L}_z t)\mathbf{K}(\varphi,0)\mathbf{U}_F(\varphi,t)= \\
&i\omega_{\mathrm{r}}\mathbf{L}_z\exp(i\omega_{\mathrm{r}}\mathbf{L}_z t)\mathbf{U}_F(\varphi,t)+\exp(i\omega_{\mathrm{r}}\mathbf{L}_z t)\left(\frac{\partial}{\partial t}\mathbf{U}_F(\varphi,t)-\mathbf{K}(\varphi,0)\mathbf{U}_F(\varphi,t)\right)= \\
&\exp(i\omega_{\mathrm{r}}\mathbf{L}_z t)\left(\frac{\partial}{\partial t}\mathbf{U}_F(\varphi,t)-(\mathbf{K}(\varphi,0)-i\omega_{\mathrm{r}}\mathbf{L}_z)\mathbf{U}_F(\varphi,t)\right)= \\
&\exp(i\omega_{\mathrm{r}}\mathbf{L}_z t)\left(\frac{\partial}{\partial t}\mathbf{U}_F(\varphi,t)-\mathbf{K}_F(\varphi)\mathbf{U}_F(\varphi,t)\right)
\end{aligned}
$$

this leads to a directly solvable Equation (A.7)

$$
\frac{\partial}{\partial t}\mathbf{U}_F(\varphi,t)=\mathbf{K}_F(\varphi)\mathbf{U}_F(\varphi,t) \tag{A.7}
$$

We defined the Floquet transmission operator as $\mathbf{K}_F(\varphi)=\mathbf{K}(\varphi,0)-i\omega_{\mathrm{r}}\mathbf{L}_z$. The Floquet transmission operator is the constant transmission operator $\mathbf{K}(\varphi,0)$ with a correction for the rotation - $i\,\omega_r\,\mathbf{L}_z$. Equation (A.7) provides a solution for the Floquet evolution operator, $\mathbf{U}_F(\varphi,t)=\exp(\mathbf{K}_F(\varphi)t)$.

Using the transformed Equation (A.7), the solution of Equation (A.4) will be

$$
\begin{aligned}
v(\varphi,t)&=\mathbf{U}(\varphi,t)v_0 \\
&=\exp(i\omega_{\mathrm{r}}\mathbf{L}_z t)\mathbf{U}_F(\varphi,t)v_0 \\
&=\exp(i\omega_{\mathrm{r}}\mathbf{L}_z t)\exp(\mathbf{K}_F(\varphi)t)v_0
\end{aligned}
\tag{A.8}
$$

This is the operator presentation of the Floquet solution.

Because the Floquet transmission operator contains only the operator $\mathbf{L}_z$ and $\mathbf{F}_p$, the eigenvalues λ_i and eigenstates $\psi_i(\varphi)$ of $\mathbf{K}_F$ can be calculated numerically. The initial state should be expressed in terms of these eigenstates:

$$v_0 = \sum_i v_{0i}\psi_i(\varphi). \tag{A.9}$$

In part B (Equation B.7) it is shown that the eigen-states $\psi_i(\varphi)$ can be expanded in terms of Fourier states, $f_{il}\,\Phi_l(\varphi)$,

$$v_0 = \sum_i \sum_{l=-\infty}^{\infty} v_{0i} f_{il} \Phi_l(\varphi). \tag{A.10}$$

where f_{il} is the l^{th} Fourier coefficient of the Fourier expansion for the i^{th} eigen-state. Substitution of Equation (A.10) in Equation (A.3) gives

$$\begin{aligned} & v(\varphi_0,t) \\ &= \sum_{m=-\infty}^{\infty} \tfrac{1}{\sqrt{2\pi}} \exp(-im\varphi_0) \int_{-\pi}^{\pi} \left(\exp(i\omega_r \mathbf{L}_z t) \left(\sum_i \exp(\mathbf{K}_F(\varphi)t) v_{0i}\psi_i(\varphi) \right) \right) \Phi_m(\varphi) d\varphi \\ &= \sum_{n=-\infty}^{\infty} \tfrac{1}{\sqrt{2\pi}} \exp(in\varphi_0) \int_{-\pi}^{\pi} \left(\left(\sum_i \exp(\lambda_i t) \sum_{l=-\infty}^{\infty} \exp(i\omega_r l t) v_{0i} f_{il} \Phi_l(\varphi) \right) \right) \Phi_{-n}(\varphi) d\varphi \\ &= \tfrac{1}{\sqrt{2\pi}} \sum_{n=-\infty}^{\infty} \sum_i v_{0i} f_{in} \exp(in(\varphi_0 + \omega_r t)) \exp(\lambda_i t) \end{aligned} \tag{A.11}$$

which is analogue to the Shirley formula [66]. In the derivation the eigenvalue equation of the angular momentum operator (B.5) and the orthonormality of the Fourier states (B.7) are applied. Equation (A.1) is now given in terms of Fourier coeffients, f_{il}, and Floquet exponents, λ_i.

From this equation the dominant eigenvalue λ_{max} can be obtained, which determines the stability of the infection-free equilibrium. If the real part of dominant eigenvalue λ_{max} is larger than 0, long term growth of the infected population will occur, while when the real part λ_{max} is smaller than 0, the size of the infected population will fluctuate but finally becomes zero.

In Part C, we will give an example for the calculation of the dominant eigen-value, and some considerations.

Part B: Operators and functions for the description of rotations

In part B, we will show the operators and functions used to describe the rotations. We will give the definition of an angular momentum operator $\mathbf{L}_z$, and the Fourier operator, $\mathbf{F}_p$. By showing their commutation relation, we will show that a transform is possible of the Fourier operator. This property is used in (A.6). The eigen-states of angular momentum operator $\mathbf{L}_z$ are the Fourier states. They are used to describe the Fourier expansion of a function and this is used in (A.10). The Fourier operators appeared to be orthonormal and that is used in (A.11). Furthermore, the transform for the initial phase value φ_0 to a phase variable φ is shown to be another example of expressing the Dirac Delta function in terms of Fourier states. This property is used in (A.3) and (A.11).

The periodicity described by Fourier states and the Angular Momentum.

For our approach it is necessary to know the periodicity of the system. The periodicity is introduced in our case by the rotation of the earth around the sun, hence the periodicity ω_r of the system is known. We describe the rotation of the earth around the

sun in physical terms by an angular momentum operator $\mathbf{L}_z$, which is an infinitesimal rotation in the plane perpendicular to the z-axis, according to [69].

$$\mathbf{L}_z = -i\frac{\partial}{\partial\varphi}. \tag{B.1}$$

In addition to the angular momentum operator we define the Fourier operator [67]

$$\mathbf{F}_p = \exp(ip\varphi). \tag{B.2}$$

$\mathbf{L}_z$ and $\mathbf{F}_p$ have the following relation

$$\begin{aligned}\mathbf{L}_z\mathbf{F}_p\psi &= \left(-i\frac{\partial}{\partial\varphi}\right)\exp(ip\varphi)\psi \\ &= p\exp(ip\varphi)\psi + \exp(ip\varphi)\left(-i\frac{\partial}{\partial\varphi}\right)\psi \\ &= \mathbf{F}_p(p+\mathbf{L}_z)\psi\end{aligned} \tag{B.3}$$

in which ψ is an arbitrary state. This relation has as a consequence the following transformation property

$$\begin{aligned}\exp(i\omega_r\mathbf{L}_z t)\mathbf{F}_p\exp(-i\omega_r\mathbf{L}_z t)\psi &= \left(\sum_{j=0}^{\infty}\frac{(i\omega_r)^n}{n!}(\mathbf{L}_z)^n\right)\mathbf{F}_p\exp(-i\omega_r\mathbf{L}_z t)\psi \\ &= \mathbf{F}_p\left(\sum_{j=0}^{\infty}\frac{(i\omega_r)^n}{n!}(p+\mathbf{L}_z)^n\right)\exp(-i\omega_r\mathbf{L}_z t)\psi \\ &= \mathbf{F}_p\exp(ip\omega_r t)\exp(i\omega_r\mathbf{L}_z t)\exp(-i\omega_r\mathbf{L}_z t)\psi \\ &= \mathbf{F}_p\exp(ip\omega_r t)\psi\end{aligned} \tag{B.4}$$

In this derivation we use the expansion of an exponential function, Equation (B.3) en de property $\exp(i\omega_r\mathbf{L}_z t)\exp(-i\omega_r\mathbf{L}_z t) = 1$. The eigenvalue equation of this angular momentum operator is [67, 69]

$$\mathbf{L}_z\Phi_l(\varphi) = l\Phi_l(\varphi), \tag{B.5}$$

in which the eigen-states are Fourier states $\Phi_l(\varphi) = \frac{1}{\sqrt{2\pi}}\exp(il\varphi)$, which have the property $\Phi_l^*(\varphi) = \frac{1}{\sqrt{2\pi}}\exp(-il\varphi) = \Phi_{-l}(\varphi)$. When the Fourier operator $\mathbf{F}_p$ is applied to the F, the Fourier states

$$\begin{aligned}\mathbf{F}_p\Phi_l(\varphi) &= \tfrac{1}{\sqrt{2\pi}}\exp(ip\varphi)\exp(il\varphi) \\ &= \Phi_{l+p}(\varphi)\end{aligned} \tag{B.6}$$

cause an increase in the order of the function, i.e. transform *l* into *l*+*p*.

Fourier expansion

For an arbitrary function *f*(φ) of this φ holds $f(\varphi) = f(\varphi + 2\pi k)$ with *k* an integer. This implies that this function could be expanded in terms of the Fourier states similar to a Fourier expansion [68].

$$\begin{aligned}f(\varphi) &= \sum_{l=-\infty}^{\infty} f_l\Phi_l(\varphi) \\ f_l &= \int_{-\pi}^{\pi} f(\varphi)\Phi_l^*(\varphi)d\varphi\end{aligned} \tag{B.7}$$

In the case of $f(\varphi)=\Phi_n(\varphi)$, the coefficients f_l equal the Delta function δ_{nl}, which is 1 for n=l and 0 otherwise. This means that the Fourier states are normalized.

Transform of the initial phase to the phase variable
The unit impulse or Dirac Delta function is used in Equation (A.3) to transform the initial phase into a variable and in Equation (A.11) for the back transformation [68]. This function is defined by its transformation property of an arbitrary function g

$$\int_{-\pi}^{\pi} g(\varphi)\delta(\varphi-\varphi_0)d\varphi = g(\varphi_0) \tag{B.8}$$

This Dirac Delta function can also be expressed in terms of the Fourier states using the Fourier expansion

$$\begin{aligned}\delta(\varphi-\varphi_0) &= \sum_{m=-\infty}^{\infty}\left(\int_{-\pi}^{\pi}\delta(\varphi-\varphi_0)\Phi_m^*(\varphi)d\varphi\right)\Phi_m(\varphi)\\ &= \sum_{m=-\infty}^{\infty}\tfrac{1}{\sqrt{2\pi}}\exp(-im\varphi_0)\Phi_m(\varphi)\end{aligned} \tag{B.9}$$

Part C: A numerical example
The simplest periodic model of a vector-borne infection describes one vector population and one host population, in which all parameters are time independent with exception of the transmission rate, *b(t)*. For such a model, Equation (A.1) has the form,

$$\begin{aligned}\frac{\partial}{\partial t}v(\varphi_0,t) &= \mathrm{K}(\varphi_0,t)v(\varphi_0,t)\\ \frac{\partial}{\partial t}\begin{pmatrix}x(\varphi_0,t)\\ y(\varphi_0,t)\end{pmatrix} &= \begin{pmatrix}-\mu_x & \frac{b(t)}{N_h}\\ b(t) & -\mu_y\end{pmatrix}\begin{pmatrix}x(\varphi_0,t)\\ y(\varphi_0,t)\end{pmatrix}\end{aligned} \tag{C.1}$$

in which x and y are infected vectors and hosts, and μ_x is vector mortality and μ_y is host mortality. In this example the transmission rate is the following function:

$$b(t) = {}^1\!/_2 + {}^1\!/_4\,(\sin(2\,\pi\,t) - \sin(3\,\pi\,t)) \tag{C.2}$$

The final result in Equation (A.11) is the characteristic equation that needs to be solved. This can be done by first expanding the transmission operator **K** into Fourier states using (B.7).

$$\mathbf{K} = \sum_{l=-\infty}^{\infty}\mathbf{M}_l \tag{C.3}$$

For our example, this means that we have to expand Equation (C.2) in Fourier series. Equations (B.7) and (A.11) seem to need an infinite expansion. Due to the fact that Equation (C.2) only has fluctuations with 2 π and 3 π, the Fourier series has only 7 terms.

$$b(t) = {}^{1}/_{2} + {}^{1}/_{4}\left(\sin(2\,\pi\,t) - \sin(3\,\pi\,t)\right) = \sum_{l=-\infty}^{\infty} f_l\ \Phi_i(\varphi) = \sum_{l=-3}^{3} -i\sqrt{2^{-(1+\pi)-(5-\pi)}}\, e^{li\pi t} \qquad \text{(C.4)}$$

For Equation (C.2) it is evident that the Fourier series has a maximum length of 7 (l = -3 to 3). Extra terms will not add anything, hence expansion to this length is equal to an expansion to infinity. Expanding Matrix **K** to a 2 n +1 length Fourier series will result in 2 n + 1 matrices of Fourier coefficients, f_{il}, which we denote here by $\mathbf{M}_l$ in Equation (C.5), where we expand Matrix **K** to $\mathbf{M}_{-3}$ until $\mathbf{M}_3$.

However, for more complex functions the Fourier expansion requires us to cut-off the expansion at some arbitrary length of expansion. The cut-off should be chosen such that the finite Fourier series approximates the real function with enough precision for the particular model one is working with. The length of the series will, however, increase the computational time, therefore precision and performance need to be balanced.

The second decision is to cut-off the number of eigen-states to include in the calculation (subscript i of the summation in Equation A.9). Increasing the number of eigen-states will increase the precision of the calculation, but also requires more computational power. Again precision and performance have to be balanced. The number of eigen-states can be determined by running the model with increasing k number of eigen states for a few example parameter sets. If the next number of eigen states (k+1) does not change the outcome more than p for k eigen states, k eigenstates were used. We used p = 0.001, which came down to k = 3 for the example.

In our example, using a Fourier series of order 3 and using 3 eigen-states, will give the following matrix C.5:

$$\begin{vmatrix} M_0 - & M_1 & M_2 & M_3 & 0 & 0 & 0 \\ M_{-1} & M_0 - & M_1 & M_2 & M_3 & 0 & 0 \\ M_{-2} & M_{-1} & M_0 - & M_1 & M_2 & M_3 & 0 \\ M_{-3} & M_{-2} & M_{-1} & M_0 & M_1 & M_2 & M_3 \\ 0 & M_{-3} & M_{-2} & M_{-1} & M_0 + & M_1 & M_2 \\ 0 & 0 & M_{-3} & M_{-2} & M_{-1} & M_0 + & M_1 \\ 0 & 0 & 0 & M_{-3} & M_{-2} & M_{-1} & M_0 + \end{vmatrix} \qquad \text{(C.5)}$$

Diagonalization of this matrix (C.5) and calculation of the eigenvalues of this matrix will provide the Floquet exponents. If the largest of these exponents is larger than 0,

the infection-free equilibrium is unstable. From this we conclude that the infection will persist.